2006-15

Final Report

Investigation of the Low-Temperature Fracture Properties of Three MnROAD Asphalt Mixtures

MINNESOTA DEPARTMENT OF TRANSPORTATION

LRRB
LOCAL
ROAD RESEARCH
BOARD

Research
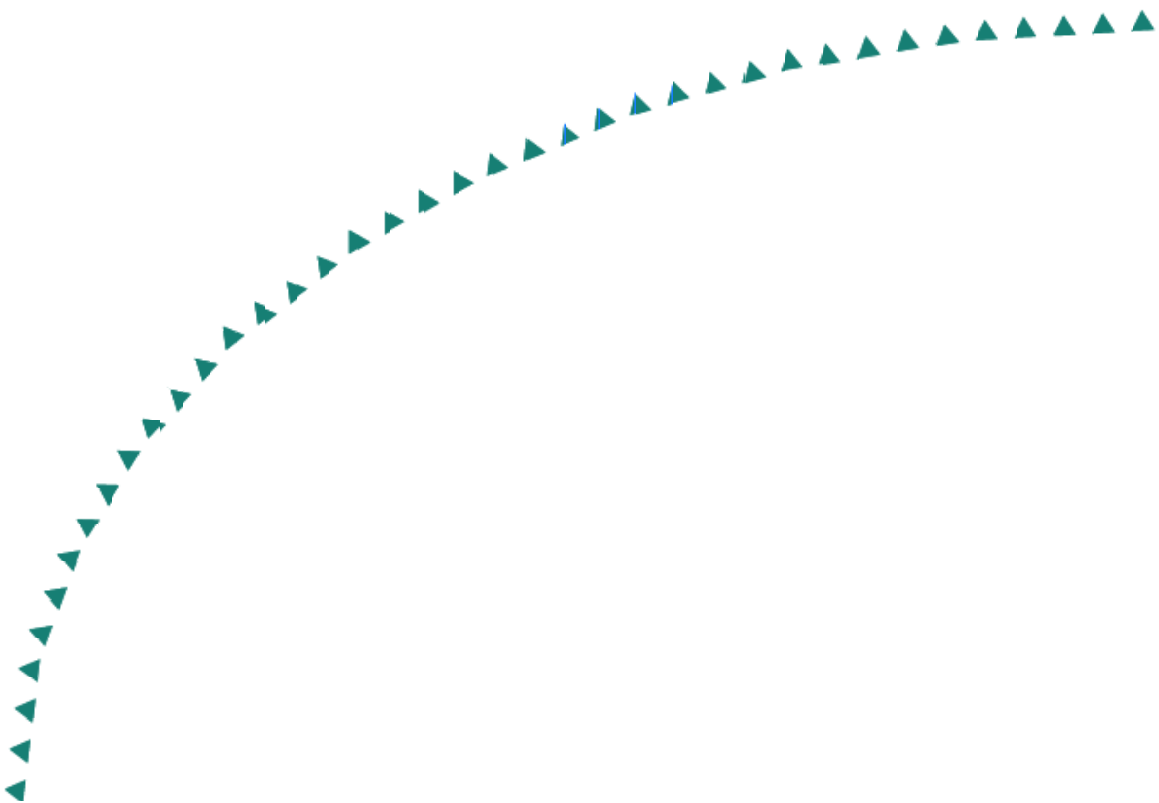
Technical Report Documentation Page

1. Report No. MN/RC-2006-15	2.	3. Recipients Accession No.
4. Title and Subtitle Investigation of the Low-Temperature Fracture Properties of Three MnROAD Asphalt Mixtures		**5. Report Date** May 2006
		6.
7. Author(s) Xinjun Li, Adam Zofka, Xue Li, Mihai Marasteanu, Timothy R. Clyne		**8. Performing Organization Report No.**
9. Performing Organization Name and Address Department of Civil Engineering University of Minnesota 500 Pillsbury Dr. S.E. Minneapolis, MN 55455		**10. Project/Task/Work Unit No.**
		11. Contract (C) or Grant (G) No. (c) 81655 (wo) 108
12. Sponsoring Organization Name and Address Minnesota Department of Transportation Office of Research Services 395 John Ireland Boulevard Mail Stop 330 St. Paul, Minnesota 55155		**13. Type of Report and Period Covered** Final Report
		14. Sponsoring Agency Code

16. Abstract (Limit: 200 words)

In this research effort, field cores were taken from cells 33, 34 and 35 at the MnROAD facility to determine the fracture properties of the field mixtures, to compare them with the laboratory-prepared mixtures analyzed in a previous study, and to evaluate the effect of aging at different depths in the asphalt layer. In addition, the properties of the recovered binders from the field cores as well as the properties of the original binders aged in laboratory conditions were investigated.

The test results and the analyses performed indicate that the fracture tests performed on asphalt binders and asphalt mixtures have the potential to predict the field performance of asphalt pavements with respect to thermal cracking. The binder results confirm the predictions of the current performance grading system; however, it appears that the fracture resistance of the PG-34 asphalt mixture is better than the fracture resistance of the PG-40 mixtures, which is the opposite of what the PG system predicts.

17. Document Analysis/Descriptors asphalt binder, asphalt mixture, fracture energy, fracture toughness, PG system, aging, Superpave, field performance, low temperature cracking		**18. Availability Statement** No restrictions. Document available from: National Technical Information Services, Springfield, Virginia 22161	
19. Security Class (this report) Unclassified	**20. Security Class (this page)** Unclassified	**21. No. of Pages** 74	**22. Price**

INVESTIGATION OF THE LOW-TEMPERATURE FRACTURE PROPERTIES OF THREE MnROAD ASPHALT MIXTURES

Final Report

Prepared by:

Xinjun Li
Adam Zofka
Xue Li
Mihai O. Marasteanu
Timothy R. Clyne

University of Minnesota
Department of Civil Engineering

May 2006

ACKNOWLEDGEMENTS

TABLE OF CONTENTS

LIST OF TABLES

LIST OF FIGURES

EXECUTIVE SUMMARY

In a previous research effort sponsored by MnDOT, the fracture properties of asphalt mixtures used in the construction of cells 33, 34 and 35 of the MnROAD facility were determined using a new experimental protocol based on a Semi Circular Bend (SCB) test. In recent years, a number of research efforts have shown that the field compacted asphalt mixture samples are different than the Superpave Gyratory Compactor (SGC) laboratory compacted asphalt mixture specimens. In addition, the effects of aging play a critical role in the fracture resistance of field asphalt mixtures.

In this research effort, field cores were taken from cells 33, 34 and 35 at the MnROAD facility to determine the fracture properties of the field mixtures, to compare them with the laboratory-prepared mixtures, and to evaluate the effect of aging at different depths in the asphalt layer. In addition, the binders were extracted and recovered from the 25 mm slices cut along the depth of the cores. The properties of the recovered binders as well as the properties of the original binders aged in laboratory conditions were investigated, using standard testing procedures part of the current specifications as well as additional test methods.

The analysis of the mixture experimental results indicates that the fracture energy of the field samples is significantly affected by the temperature and the type of binder used, while the fracture toughness of the field samples is significantly affected only by the type of binder used. The comparison between the field samples and the laboratory specimens shows that the fracture energy of the field samples is lower than the fracture energy of the laboratory specimens and the fracture toughness of the field samples is lower than the fracture energy of the laboratory specimens. However, the evolutions of the fracture toughness and fracture energy with type of binder and temperature are similar for the field samples and laboratory specimens. The difference in properties with the location within the pavement does not indicate a consistent pattern although in some cases the surface seemed to be less cracking-resistant (possibly indicating more aging) than the middle and the bottom layer.

The analysis of the experimental data obtained from tests performed on the binders recovered from cores and on the laboratory-aged original binders indicates that the properties of the field binders are different than the laboratory-aged binders. In particular, significant differences are noticed in the phase angle master curves. At low temperatures, the most

significant change is observed in the m-value limiting temperatures, which clearly indicates a substantial change in the relaxation properties of the recovered binder compared to the laboratory-aged binder in spite of the less significant change in stiffness. The difference in properties with the location within the pavement did not follow a consistent pattern although in some cases the surface seemed to be stiffer (possibly indicating more aging) than the middle and the bottom layer.

The limited low temperature distress data collected at MnROAD indicates the fracture tests performed on asphalt binders and asphalt mixtures have the potential to predict the field performance of asphalt pavements with respect to thermal cracking. The binder and mixture fracture toughness results indicate that cells 34 and 35 have better fracture resistance than cell 33, and the mixture results suggest that cell 34 has better resistance than cell 35, which is the opposite of what the PG system predicts.

CHAPTER 1

INTRODUCTION

Background

In a previous research effort sponsored by MnDOT, the fracture properties of asphalt mixtures used in the construction of cells 33, 34 and 35 of the MnROAD facility were determined using a new experimental protocol based on a Semi Circular Bend (SCB) test. In this previous study the original loose mix was compacted to the desired parameters in the laboratory using the Superpave gyratory compactor (SGC), and 1" thick test specimens were cut from the SGC specimen.

In recent years, a number of research efforts have shown that the field-compacted asphalt mixture samples are different than the SGC laboratory-compacted asphalt mixture specimens. In addition, the effects of aging play a critical role in the fracture resistance of field asphalt mixtures. To date, there is little agreement with respect to the magnitude of the depth, from the asphalt pavement surface, at which aging effects are still significant.

In this research effort, field cores were taken from cells 33, 34 and 35 at the MnROAD facility to determine the fracture properties of the field mixtures and to evaluate the effect of aging with depth. To better understand the relationship between the properties of these mixtures and the field performance, the historical data on these three cells needs to be documented.

Chapter 1 documents the history and performance of the aforementioned MnROAD cells. Most of the information contained in this task was provided by Ben Worel, with assistance from Ron Mulvaney and other MnROAD staff.

MnROAD Layout

The Minnesota Department of Transportation (Mn/DOT) constructed the Minnesota Road Research Project (MnROAD) between 1990 and 1994. MnROAD is an extensive pavement research facility consisting of two separate roadway segments: the Mainline Test Road (Mainline) and Low Volume Road (LVR), containing a total of 51 distinct test cells. Each MnROAD test cell is approximately 500 feet long. The subgrade, aggregate base, and surface materials as well as the roadbed structure and drainage methods vary from cell to cell. The layout and the designs used for the cells part of the LVR are shown in Figure 1.1.

Figure 1.1. MnROAD Test Cell Layout (Low Volume Road)

Cells 33, 34, are part of the 20 test cells located on the LVR, a 2-lane, 2 ½-mile closed loop component of MnROAD. The traffic on the LVR is restricted to a MnROAD operated vehicle, an 18-wheel, 5-axle, tractor/trailer, with two different loading configurations. The "heavy" load has a gross vehicle weight of 102 kips (102K configuration). The "legal" load has a gross vehicle weight of 80 kips (80K configuration). The tractor/trailer travels on the inside lane of the LVR loop in the 80K configuration on all weekdays except for Wednesdays when the

2

tractor/trailer operates in the 102K configuration and travels in the outside lane of the LVR loop. This arrangement results in an approximately equal number of ESALs for the two lanes. The number of ESALs on the LVR is determined by the number of laps (80 per day) for each day; the data is entered and stored in the MnROAD database.

Construction and Materials

Cell 33, 34 and 35 were originally constructed as aggregate cells. In 1999 the three cells were reconstructed to verify the current Superpave criteria related to low temperature cracking (thermal and/or transverse cracking). Each test cell used the same mix design for the 4" layer of Superpave mixture placed over a 12" Class-6 Special aggregate base. The only difference between the three cells was the grade of asphalt binder used. It was believed that this pavement structure would not fail due to fatigue cracking and therefore it would allow thermal cracks to develop first. The design was based on a 20-year ESAL of 375,000.

The Class 6 Special aggregate base was chosen based on past experience at MnROAD which indicated that this base material induced more thermal cracks in the HMA pavements as compared to other types of aggregates. This is based on past performance of the 1993 LVR test cells. Class 6 base contains a minimum 15 percent crushed stone and less than 7 percent shale.

The Superpave PG binders used in the three cells were PG 58-28 (cell 33), PG 58-34 (cell 34), and PG 58-40 (cell 35). Note that each of these binders has the same high limit temperature value of 58°C, but the low limit temperature value varies from -28°C, -34°C, and -40°C. The PG 58-34 and PG 58-40 binder are polymer-modified binders using the Stylink process: the PG 58-28 is not modified. The mix designs are shown in Figures 1.2 to 1.4.

BITUMINOUS PLANT RECOMMENDATION
Minnesota Department of Transportation
Materials and Research Laboratory
1400 Gervais Avenue
Maplewood, MN 55109
Phone: (651) 779-5614
FAX: (651) 779-5580

#0 - 990273

Date: 8/24/99

To: TIM ANDERSEN   Engineer: MN/DOT (MN/ROAD)

The mix design for Spec. 2360 (1999)   Mixture Type SPWEB240B   Is hereby approved
for this project as follows:

STATE PROJ. | 8 8 1 6 - 4 0

PLANT NO. | 9 0 0 9 0 1 - 9 9 A   JOB MIX FORMULA

Begin With Test Number

| - - N W - - - |
| S P W E 2 0 1 |

Sieve Size (mm) (in.)	Composite Formula	WARNING LIMITS			JMF LIMITS			For Information Only Virgin Formula
37.5 (1 ½)			-			-		P P
25.0 (1)			-			-		E A
19.0 (3/4)	100	-	-	-	100	-	100	R S
12.5 (1/2)	94	-	-	-	90	-	100	C S
9.5 (3/8)	86	-	-	-	79	-	90	E I
4.75 (#4)	66	-	-	-	59	-	73	N N
2.36 (#8)	54	-	-	-	48	-	58	T G
0.075 (#200)	4.7	-	-	-	2.7	-	6.7	
Spec. Voids	4.0	-	-	-	2.7	-	5.3	%AC (NEW)
Spec. VMA	14.0	-			13.7			

| %AC | 5.8 | - | 5.4 |

%AC (TOTAL)   MIN

TM# 0- 99108 Indicates a Gyratory Density of 2404.4 (150.1) kg/m^3 (lbs/ft^3) at 75 Design Gyrations
Use of anti-strip agent required NO

Proportions		Source of Material	Sp.G
12	%	DANNER 3/4" CLASS D ROCK	2.696
20	%	DANNER 1/2" CLASS D ROCK	2.679
23	%	DANNER CRUSHED FINES	2.637
45	%	OTTO PED SAND	2.622
	%		
	%		
	%		

Mix Aggregate Specific Gravity at the Listed Percentages = 2.645
Remarks: LAB MIXING TEMP. RANGE = 288 - 297°F   LAB COMPACTION TEMP. RANGE = 267 - 275°F
NOTE: TEMPERATURES ARE FOR PG 58-28 KOCH (1999) AC. TEMPERATURES ARE FOR LAB INFORMATION ONLY.

Mix Design approved by:
Thomas T. Hunt
Mix Design Specialist

cc:
Dist. Mat'ls Eng. (Dist. 5 &9) (2)
Metro Inspection
Contractor – BITUMINOUS ROADWAYS #1

Figure 1.2. Cell 33 (PG 58-28) Mix Design

BITUMINOUS PLANT RECOMMENDATION
Minnesota Department of Transportation
Materials and Research Laboratory
1400 Gervais Avenue
Maplewood, MN 55109
Phone: (651) 779-5614
FAX: (651) 779-5580

#0 - 990274

Date: 8/24/99

To: TIM ANDERSEN

Engineer: MN/DOT (MN/ROAD)

The mix design for Spec. 2360 (1999) for this project as follows:

Mixture Type SPWEB240C Is hereby approved

STATE PROJ. **8 8 1 6 - 4 0**

PLANT NO. **9 0 0 9 0 1 - 9 9 A**   JOB MIX FORMULA

Begin With Test Number

`- - N W - - -`

`S P W E 3 0 1`

Sieve Size (mm) (in.)	Composite Formula	WARNING LIMITS			JMF LIMITS			For Information Only Virgin Formula		
37.5 (1 ½)			-			-		P	P	
25.0 (1)			-			-		E	A	
19.0 (3/4)	100	-	-	-	100	-	100	R	S	
12.5 (1/2)	94	-	-	-	90	-	100	C	S	
9.5 (3/8)	86	-	-	-	79	-	90	E	I	
4.75 (#4)	66	-	-	-	59	-	73	N	N	
2.36 (#8)	54	-	-	-	48	-	58	T	G	
0.075 (#200)	4.7	-	-	-	2.7	-	6.7			
Spec. Voids	4.0	-	-	-	2.7	-	5.3	%AC		
Spec. VMA	14.0	-			13.7			(NEW)		

%AC **5.8** - %AC (TOTAL)   **5.4** MIN

TM# 0- 99108 Indicates a Gyratory Density of **2404.4 (150.1)** kg/m³ (lbs/ft³) at **75** Design Gyrations
Use of anti-strip agent required **NO**

Proportions		Source of Material	Sp.G
12	%	DANNER 3/4" CLASS D ROCK	2.696
20	%	DANNER 1/2" CLASS D ROCK	2.679
23	%	DANNER CRUSHED FINES	2.637
45	%	OTTO PED SAND	2.622
	%		
	%		
	%		

Mix Aggregate Specific Gravity at the Listed Percentages = 2.645
Remarks: LAB MIXING TEMP. RANGE = 275 - 287°F   LAB COMPACTION TEMP. RANGE = 240 - 246°F
NOTE: TEMPERATURES ARE FOR PG 58-34 KOCH (1999) AC. TEMPERATURES ARE FOR LAB INFORMATION ONLY.

Mix Design approved by:
Thomas T. Hunt
Mix Design Specialist

cc:
Dist. Mat'ls Eng. (Dist. 5 &9) (2)
Metro Inspection
Contractor – BITUMINOUS ROADWAYS #1

Figure 1.3. Cell 34 (PG 58-34) Mix Design

BITUMINOUS PLANT RECOMMENDATION
Minnesota Department of Transportation
Materials and Research Laboratory
1400 Gervais Avenue
Maplewood, MN 55109
Phone: (651) 779-5614
FAX: (651) 779-5580

#0 - 990275

Date: 8/24/99

To: TIM ANDERSEN

Engineer: MN/DOT (MN/ROAD)

The mix design for Spec. 2360 (1999) for this project as follows:

Mixture Type SPWEB240D Is hereby approved

STATE PROJ. | 8 8 1 6 - 4 0

PLANT NO. | 9 0 0 9 0 1 - 9 9 A | JOB MIX FORMULA

Begin With Test Number
| - | - | N | W | - | - | - |
| S | P | W | E | 4 | 0 | 1 |

Sieve Size (mm) (in.)	Composite Formula	WARNING LIMITS			JMF LIMITS			For Information Only Virgin Formula
37.5 (1 ½)			-			-		P E R C E N T
25.0 (1)			-			-		P A S S I N G
19.0 (3/4)	100	-	-	-	100	-	100	
12.5 (1/2)	94	-	-	-	90	-	100	
9.5 (3/8)	86	-	-	-	79	-	90	
4.75 (#4)	66	-	-	-	59	-	73	
2.36 (#8)	54	-	-	-	48	-	58	
0.075 (#200)	4.7	-	-	-	2.7	-	6.7	
Spec. Voids	4.0	-	-	-	2.7	-	5.3	%AC (NEW)
Spec. VMA	14.0	-			13.7			

| %AC | 5.8 | - | 5.4 |
| | %AC (TOTAL) | | MIN |

TM# 0- | 99108 | Indicates a Gyratory Density of | 2404.4 (150.1) | kg/m³ (lbs/ft³) at | 75 | Design Gyrations

Use of anti-strip agent required | NO

Proportions		Source of Material	Sp.G
12	%	DANNER 3/4" CLASS D ROCK	2.696
20	%	DANNER 1/2" CLASS D ROCK	2.679
23	%	DANNER CRUSHED FINES	2.637
45	%	OTTO PED SAND	2.622
	%		
	%		
	%		

Mix Aggregate Specific Gravity at the Listed Percentages = 2.645

Remarks: LAB MIXING TEMP. RANGE = 282 - 294°F   LAB COMPACTION TEMP. RANGE = 247 - 258°F

NOTE: TEMPERATURES ARE FOR PG 58-40 KOCH (1999) AC. TEMPERATURES ARE FOR LAB INFORMATION ONLY.

Mix Design approved by:

Thomas T. Hunt

Mix Design Specialist

cc:
Dist. Mat'ls Eng. (Dist. 5 &9) (2)
Metro Inspection
Contractor – BITUMINOUS ROADWAYS #1

Figure 1.4. Cell 35 (PG 58-40) Mix Design

The gradations of aggregate base, asphalt mixture, and aggregate shoulder are listed in Tables 1.1 to 1.3, respectively. Class 6 Special was used for the base material consisting of Class A aggregate (Original Class-6 from the stockpile area). Class-2 was used for the gravel shoulder surface consisting of Class A aggregate (Meridian Granite, St. Cloud).

Table 1.1. Aggregate Base Gradations

Sieve	Requirements		Average Field Result	# of Samples	Sample Type
	Min	Max			
1"	100	100	100		
¾"	85	100	96		
3/8"	50	70	65		
# 4	30	50	41	5	Sample from Roadway
# 10	15	30	27		
# 40	5	15	13		
# 200	0	5	5.7		

Table 1.2. Asphalt Mixture Aggregate Gradations

Sieve	Requirements		PG 58-28 Average	PG 58-34 Average	PG 58-40 Average
	Min	Max			
¾"	100	100	100	100	100
½"	90	100	92.2	93.6	93
3/8"	79	90	84.8	85.8	85.2
# 4	59	73	67.4	67.8	66.6
# 8	48	58	55.4	55.6	54.6
# 200	2.7	6.7	5.2	5.2	5.1
# of Samples			5	5	5
Sample Type			Averages for Ignition Oven and Core Extraction from Contractor and Mn/DOT samples		

Table 1.3. Aggregate Shoulder Gradations

Sieve	Requirements		Average Field Result	# of Samples	Sample Type
	Min	Max			
¾"	100	100	100		
3/8"	65	90	79		
#4	35	70	51	3	Sample from Roadway
#10	25	45	33		
#40	12	30	16		
#200	5	13	6.7		

Data Collection

The MnROAD test cells contain a large numbers of sensors that were buried in the pavements for continuous data collection. Three types of data are collected: (1) stress and strain data; (2) temperature data; (3) moisture data including the depth of frozen/thawed soil. The sensors installed in the three Superpave cells are listed in Table 1.4. A description of each sensor and of its use is given below:

TC   Thermal Couple (measures the temperature of the soil and pavement)

WM   Water Mark / Moisture Block (measures the depth of frozen/thawed soil)

TDR   Time Domain Reflectometer (measures the amount of moisture in the soil)

OS   Open Stand Pipe (measures the location of the water table)

RS   Reflectometer (measures the amount of soil moisture)

PK   Pressure Sensor (measures the amount of vertical pressure - top subgrade soil)

LE   Longitudinal Strain Gauge (measures the strain at the bottom of HMA)

PG   Pressure Gauges (measures the vertical pressure in the aggregate base)

Note: Aluminum foil tape was installed on the outside of the 102k lane under the fog line. Its purpose is to set an alarm when a thermal crack appears.

Table 1.4. Sensors Installed

Cell	Sensor Type	Number of Sensors	Number of Locations
33	TC	6	1
	PK	16	2
	TDR	5	1
	LE	4	4
	PG	6	6
	OS	1	1
34	TC	17	3
	WM	15	2
	TDR	5	2
	OS	1	1
	RS	5	1
	LE	4	4
35	TC	75	1
	TDR	45	2
	LE	14	4
	OS	1	1

Cell Performance

MnROAD researchers have monitored the test cells since they were constructed in July 1999. The results of distress surveying performed in 2003 are summarized below.

Rutting

Rutting evolution in all three Superpave test cells is shown in Table 1.5 and Figure 1.5. The measurements were taken using a six-foot straight edge. More rutting was measured in the 80K lane than the 102K lane despite the same number of ESALs in each lane. The rutting appears to be more a function of the number of passes; the inside 80K lane is driven four days per week and the 102K lane is driven one day per week, each averaging 80 laps per day. This phenomenon was also observed on the original 1994 HMA test cells on the LVR. Figure 1.5 also indicates that Cell 35 accumulated rutting more quickly than the other two cells. Even though all three binders are PG 58, their lower limits are different, which result in different temperature susceptibilities for the three binders.

Table 1.5. Rutting (6-foot Straight Edge)

Cell	80K Inside Lane		102K Outside Lane	
	Outside WP	Inside WP	Outside WP	Inside WP
33	.48"	.44"	.31"	.23"
34	.46"	.42"	.36"	.30"
35	.55"	.46"	.34"	.23"
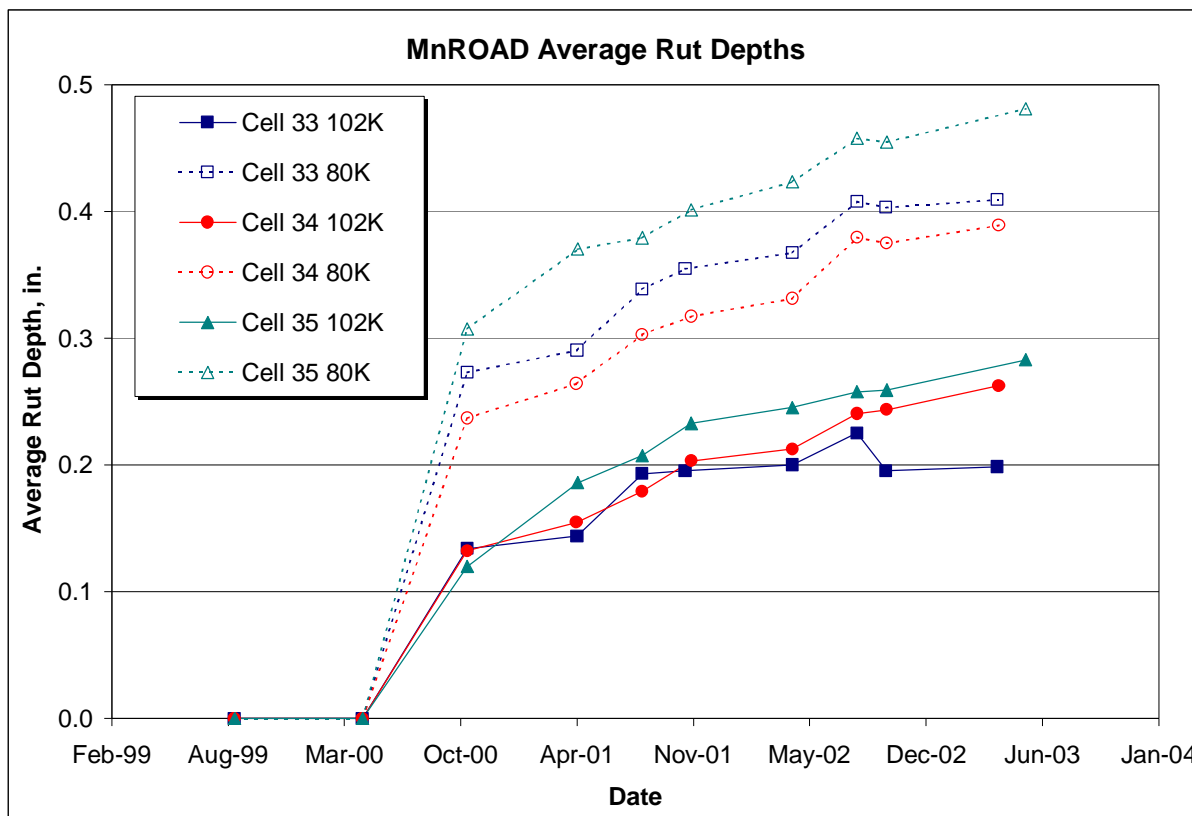
Figure 1.5. Rutting Accumulation at MnROAD

Transverse Cracking

The initial transverse cracking developed during February 2003. These cracks do not exhibit a "typical" thermal cracking pattern, which runs perpendicular to the centerline of lanes and across the entire width of both lanes. These cracks are more random in nature, as shown in Figure 1.6. Forensic observations were performed on these cracks. Two cores were taken directly on each of two cracks. The cores were debonded at the interface between two lifts. The crack could be observed in both lifts but only in one of two cores. It was very hard to decide if these random, partial-width, transverse-like cracks were due to thermal cracking.

Figure 1.6. Typical Transverse Crack in Superpave Cells

Although the 2004 crack surveying has not been completed, the preliminary data show that (1) cell 33 with binder PG 58-28 contains six full-width transverse cracks in both lanes; (2) no cracking is present in cell 34 with binder PG 58-34; (3) many little "transverse-like" cracks are visible in cell 35 with binder PG 58-40. These results seem to indicate binder PG 58-34 as the best performer of the three binders. Table 1.6 shows the amount of transverse cracks through November 2003.

Table 1.6 Transverse Cracking

Cell	80K Inside Lane		102K Outside Lane	
	Number of Cracks	**Linear Feet**	**Number of Cracks**	**Linear Feet**
33	0	0	6	13
34	0	0	0	0
35	14	66	5	24

Longitudinal Cracking

The survey also revealed the development of some longitudinal cracks, as shown in Table 1.7. A typical longitudinal crack is shown in Figure 1.7. Forensic cores taken from cell 35 showed that the cracking propagated from the top down.

Table 1.7. Longitudinal Cracking

Cell	80K Inside Lane		102K Outside Lane	
	Outside WP	Inside WP	Outside WP	Inside WP
33	0	0	0	0
34	0	0	0	0
35	2	4	3	16

Figure 1.7. Typical Longitudinal Crack in Superpave Cells

Fatigue Cracking

Cell 35 contains some fatigue cracking, as shown in Table 1.8. These cracks may have developed in areas that were not constructed to the full 4″ HMA thickness. This is consistent with observations made for the LVR test cells 27-28 when forensic cores were taken. Figure 1.8 shows a collection of the cores that were cut from Cells 33, 34, and 35. Although the three cells were designed and constructed to have a 4″ inches thick asphalt layer, the cores indicated significant variation in thickness, with values as low as 3".

Table 1.8. Fatigue Cracking

Cell	80K Inside Lane		102K Outside Lane	
	Outside WP	**Inside WP**	**Outside WP**	**Inside WP**
33	0	0	0	0
34	0	0	0	0
35	0	6 lin-ft	16 lin-ft	0

Figure 1.8. MnROAD Cores of Variable Thickness

Observed Strain Measurements

On average 80 laps were recorded each day using the MnROAD truck in the 80K lane. A typical longitudinal strain trace is shown in Figure 1.9. The strain gages are placed at the bottom of the asphalt layer (4" deep). It is obvious from the figure that the same truck loading resulted in different strain amplitudes in the three cells. The air temperature at the time of the strain measurements was 23.7°C and the pavement temperatures were as follows:

- Cell 33: 44.5°C at 1" depth and 33.9°C at 3" depth from the surface
- Cell 34: 44.9°C at 1" depth and 33.9°C at 3" depth from the surface
- Cell 33: 46.4°C at 1" depth and 37.1°C at 3" depth from the surface

This has implications for rutting and other performance in the field.
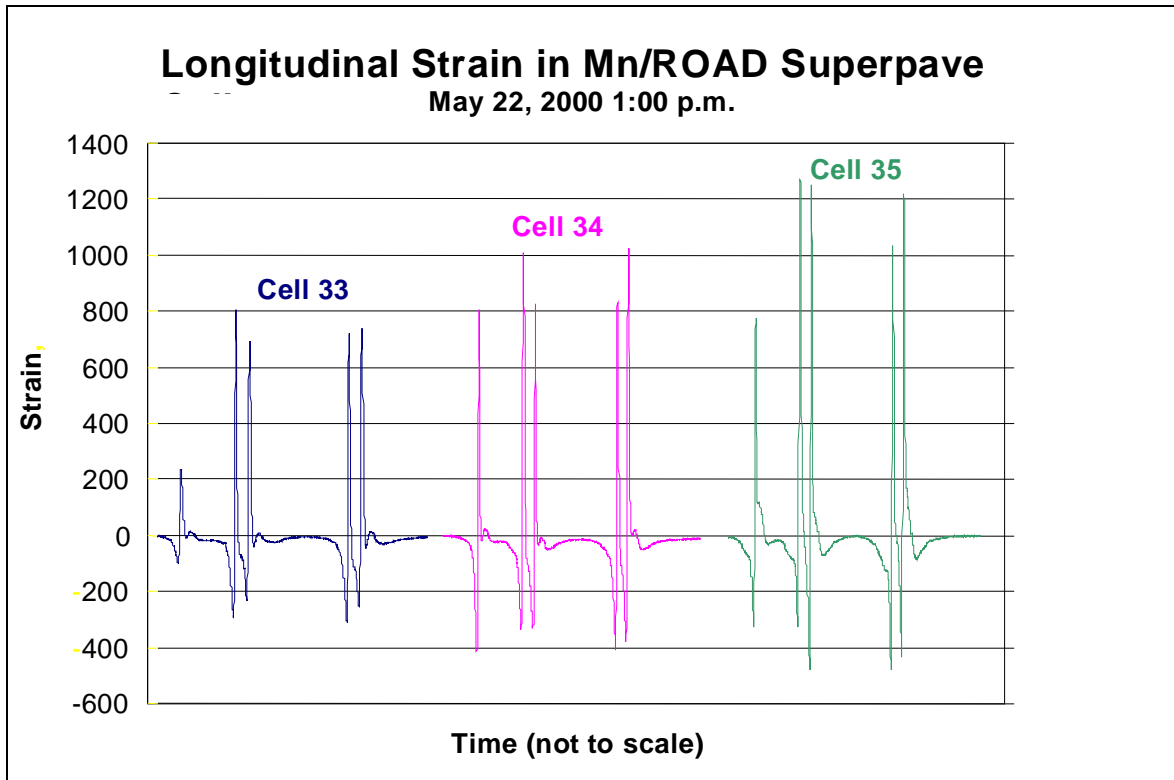
Figure 1.9. Longitudinal Strain Responses

Ride

The ride was measured with a Pathways data collection van owned by Mn/DOT. The data is used to obtain the International Roughness Index (IRI) expressed in meters/kilometer (m/km). An IRI of zero indicates a perfectly smooth pavement, while IRI values above 3.00 m/km indicate a very rough ride. The current ride index is very similar for the three cells, as shown in Table 1.9.

Table 1.9. Pathways IRI Ride Measurements (m/km)

Cell	80K Inside Lane		102K Outside Lane	
	Outside WP	**Inside WP**	**Outside WP**	**Inside WP**
33	2.23	1.91	1.33	1.50
34	2.00	2.62	1.42	1.40
35	1.96	2.10	1.83	1.96

Forensic Observations

Only one forensic activity was performed after the initial construction in 1999. The purpose of this forensic activity was to determine the source of the cracking found in cell 35.

This involved coring a transverse and longitudinal crack to determine if the crack developed from the top or the bottom of the asphalt layer. The forensic activity involved taking five cores from cell 35 on May 2, 2003. Tables 1.10 and 1.11 provide additional information on this limited forensic study.

Table 1.10. Forensic Core Locations

Core Number	TA (ft)	Offset (in)[a]	Thickness[b] (in) Lifts 1+2 =Total	Comment
3503BC001	7828	+ 48	1.75+2.125 = 3.875	On transverse crack #1 / separated at tack coat
3503BC002	7828	+ 32	2.25+2.00 = 4.25	3" off the end of transverse crack #1
3503BC003	7817	+ 28	1.75+1.50 = 3.25	On longitudinal crack in wheel path
3503BC004	7817	+ 70	2.00+2.00 = 4.00	Midlane at same station as longitudinal crack
3503BC005	7731	+ 60	2.50+1.75 = 4.25	On transverse crack #2

a. A positive offset indicates the inside 80K lane for cells 33-35.
b. Lift (1) is the bottom lift and lift (2) is the surface lift

Table 1.11. Forensic Observations

Observation Category	Observation / Comment
Thickness Variations	The cores taken at the same station as the longitudinal cracking show a ¾" difference in thickness. Air voids and density will be determined but the difference appears to be construction related due to the other cores taken in the wheel path were more consistent thickness than the one containing the longitudinal crack.
Transverse Cracks	Three cores were taken to observe the transverse cracking on two different cracks. On the first crack, one core was taken in the middle of the transverse crack and one just as it disappeared, about 3", from the end. We observed that the core taken on the transverse crack debonded between the two lifts and the crack was observed in both lifts but it appeared it developed from the surface. The bottom lift was "flexed" by hand from the top down to observe the crack better. It was noticeable but only slight at the HMA lift interface before it was broke. The second core contained no visible cracking. The second crack core showed the same as the first crack. The cracking appears to be top down. Overall the transverse cracking appears to be construction related and do not exhibit the same characteristics as traditional thermal cracks at this point.
Longitudinal Cracks	The thickness of the cores in the area of the longitudinal cracking was ¾" thinner then any of the other cores. The crack went all the way through the core and no determination of top down cracking can be made. MnROAD has observed in the past other areas on other cells that contained localized areas of "thinner" spots that eventually fatigued.

Thermal Crack Tape

Thermal crack tape was installed along the outside lane (102K) for each test cell. The tape was installed between the two HMA lifts placed on each cell. The purpose of the crack tape was to determine the exact time when a thermal crack develops. The crack tape system at MnROAD was installed in 65-ft loops (on average) that act as a continuous circuit until the continuity is broken.

As of May 2003, no surface cracks have developed through any of the thermal crack tapes installed. Each of the thermal crack tape loops remained continuous, even though the resistance has grown over time. This is caused by the expected corrosion that has developed in the sensor wires that were soldered to the crack tape foil.

CHAPTER 2

Mixture Testing

Testing Equipment and Setup

A MTS servo-hydraulic testing system was used to perform the Semi Circular Bend (SCB) tests to determine the low temperature fracture properties of the field mixtures. The SCB test is similar to the three-point bending beam test except that the SCB specimen is semicircular instead of a beam. The SCB specimen is symmetrically supported by two rollers and has a span of 120mm. Teflon paper strips were placed between the specimen and the rollers to reduce the friction on the interface. The Indirect Tension test (IDT) loading plate was used to load the SCB specimens. The load line displacement (LLD) was measured using a vertically mounted Epsilon extensometer with 38 mm gauge length. The crack mouth opening displacement (CMOD) was measured by an Epsilon clip gauge with 10 mm gauge length. The test setup is shown in Figure 2.1.
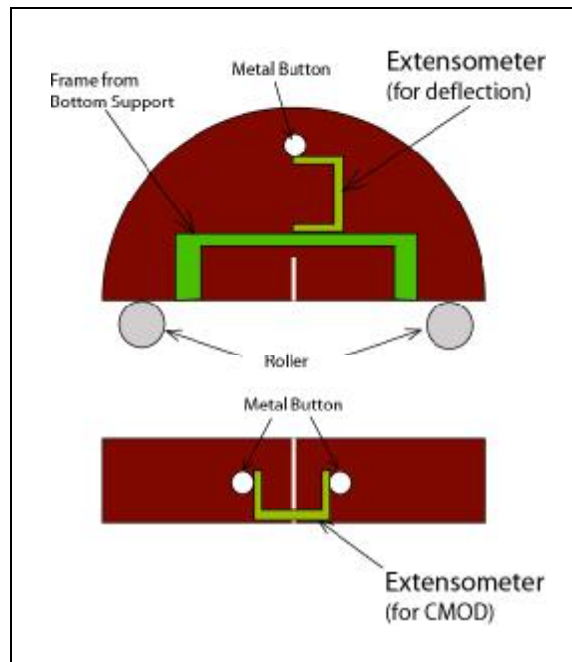
Figure 2.1. Experimental Setup

All tests were performed inside an environmental chamber. Liquid nitrogen was used to cool down the temperature. The temperature was monitored by a build-in thermocouple and an

independent Resistance Temperature Detector (RTD) with the probe attached to the mixture specimen. The chamber temperature was controlled within 1°C of the target temperature.

Prior to testing, the SCB samples were kept in the environmental chamber at the test temperature for three hours to achieve a uniform temperature field within the sample. The test was executed automatically using the MTS TestStar IIs software and the CMOD signal as the control. The CMOD rate was set to a fixed value of 0.0005mm/s. The load, the LLD and the CMOD were recorded and the load-LLD curve was plotted.

Fracture Mechanics Analysis

Fracture Toughness (K_{Ic})

The stress intensity factor (SIF), which characterizes the stress state around the crack tip, is a function of the load and the geometry:

$$K = f(P, a, W) \tag{2.1}$$

where P is the load, a is the crack length, and W is the vector of the characteristic length of the geometry. For any particular specimen, before the crack begins to propagate, the geometry is constant and the SIF changes with the change of the load at different stages. With the assumptions of LEFM, the crack begins to grow at peak load and this critical SIF is a measure of the fracture toughness of the specimen.

The Mode I critical stress intensity factor K_{IC}, also referred to as Mode I fracture toughness, K_{IC} has received considerable attention to describe the fracture resistance of asphalt materials. In this paper, K_{IC} is determined with Equation [2.2] developed by Lim et al. (1), using the value of peak load.

$$\frac{K_I}{s_0\sqrt{pa}} = Y_{I(s_0/r)} + \frac{\Delta s_0}{r}B \tag{2.2}$$

where

$\qquad K_I \qquad$ = Mode I stress intensity factor;

$\qquad s_0 \qquad = \dfrac{P}{2rt}$

$\qquad\qquad$ P = applied load;

$\qquad\qquad$ r = specimen radius;

t = specimen thickness.

Y_I = the normalized stress intensity factor

$$Y_{I(s_0/r)} = C_1 + C_2(a/r) + C_3 \exp(C_4(a/r))$$

C_i = constants;

a = notch length;

$$\frac{\Delta s_0}{r} = \frac{s_a}{r} - \frac{s_0}{r}$$

s_a, s_0 = half spans

$\dfrac{s_a}{r}$ = actual span ratio;

$\dfrac{s_0}{r}$ = nearest span ratio analyzed in the derivation of this equation (0.80, 0.67, 0.61, 0.50)

$$B = 6.55676 + 16.64035(\frac{a}{r})^{2.5} + 27.97042(\frac{a}{r})^{6.5} + 215.0839(\frac{a}{r})^{16}$$

Fracture Energy (G_f)

Another fundamental fracture property that is less dependent on the assumptions of linear elasticity and homogeneity is the fracture energy (G_f). The fracture energy was calculated according to RILEM TC 50-FMC specification (2) that has been extensively used in the study of concrete. The work of fracture (W_f) was computed as the area under the P-u curve and the fracture energy (G_f) was obtained by dividing the work of fracture with the ligament area (the product of the ligament length and the thickness of the specimen), as shown in Equation [2.3]:

$$G_f = \frac{W_f}{A_{lig}} \qquad\qquad\qquad (2.3)$$

where W_f is the work of fracture and

$$W_f = \int P du$$

A_{lig} is the area of the ligament.

With respect to the calculation of the area under the P-u curve, two issues had to be addressed. The test was started at a seating load of 0.3kN as indicated in Figure 2.2. This triangular area (O'OA in Figure 2.2) is very small and it was not included in the energy

calculation. Due to the range limitation of the extensometers all tests were stopped when the load dropped to 0.5kN. Considering that the peak load of the specimens was between 3-4kN, the tests were stopped at 12-17 percent of the peak load, which means the tail of the P-u curve cannot be experimental measured and thus the work of fracture, W_{tail}, corresponding to this part of curve cannot be calculated directly from experimental data. The W_{tail} is determined following the method described in detail elsewhere (3) and consists of the following steps:

- Fit the data to obtain the power of the curve.
- Check the power of the curve. If the power is within one standard deviation from -2, use the power from regression. If the power is outside this range use one of the two values - 2 ± 0.37 that is closer to the regressed power value.
- Calculate the tail area with the power of curve determined from above two steps.

The total work of fracture, W_{total}, the sum of the work of fracture from experimental curve (W) and the work of fracture corresponding to the tail curve (W_{tail}), is used to compute the fracture energy, G_f.
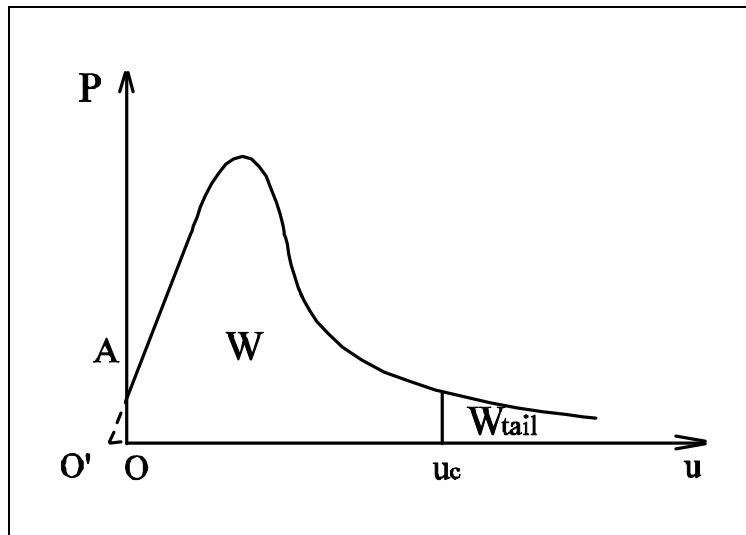
Figure 2.2. Load vs. Load-Line Displacement

Materials and Sample Preparation

As mentioned previously field cores were taken from cells 33, 34 and 35 at the MnROAD facility to determine the fracture properties of the field mixtures and to evaluate the effect of aging with depth.

The cores were taken from MnROAD in July and October 2004, approximately 5 years after the construction of the cells. Detailed information about the location and size of the cores is provided in Figure 2.3 and Table 2.1
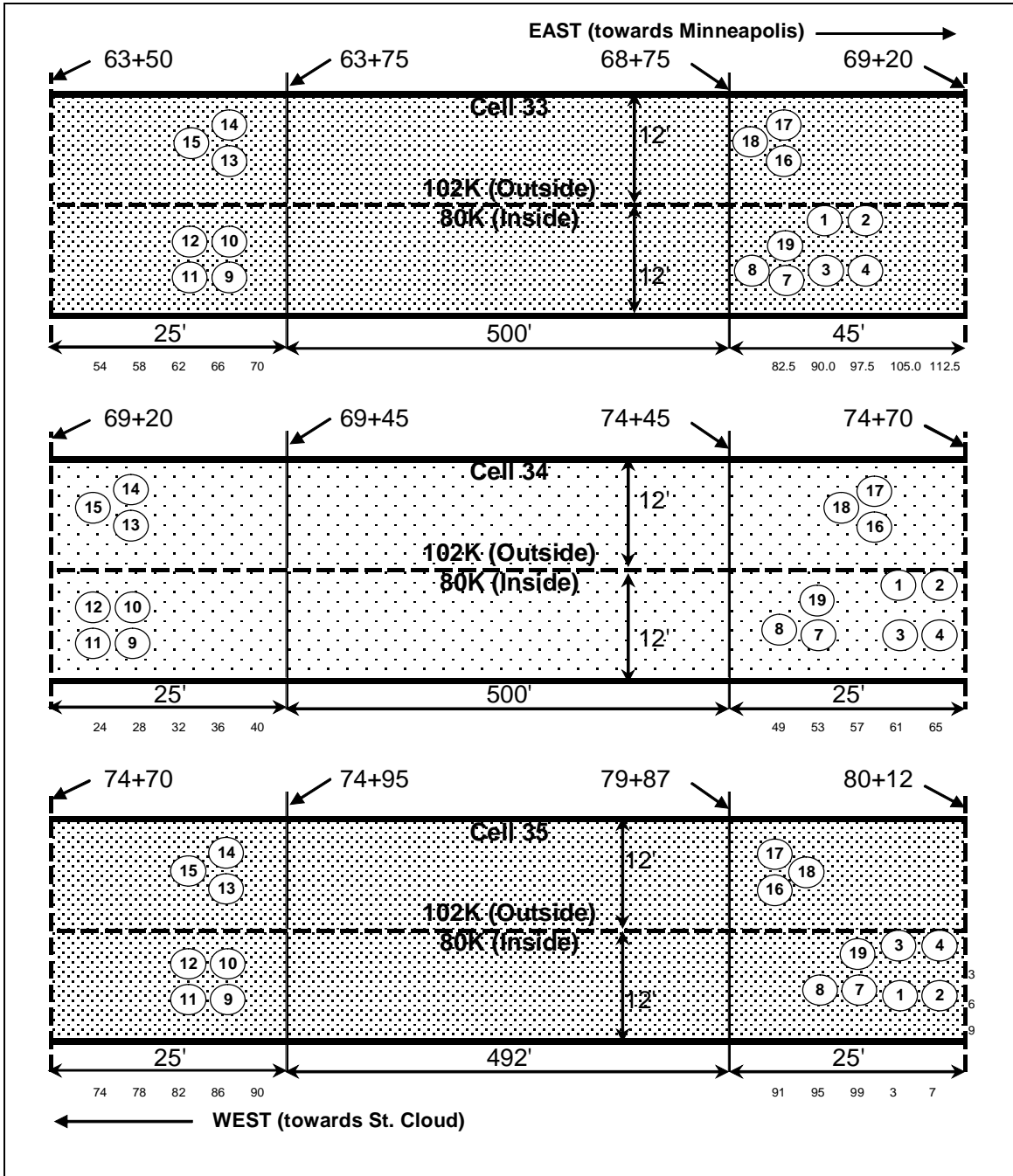
Figure 2.3. Cores location

Table 2.1. Core location and thickness

MnROAD ID	Cell 33			Cell 34			Cell 35		
	Station	Offset from center	Thickness	Station	Offset from center	Thickness	Station	Offset from center	Thickness
04BC001	**68+95**	**2.5**	**3.5**	**74+65**	**2.5**	**4**	80+07	6	4.2
04BC002	**68+97.5**	**2.5**	**3.1**	**74+67.5**	**2.5**	**3.8**	80+09.5	6	4.3
04BC003	68+95	6	3.7	74+65	6	3.3	**80+07**	**2.5**	**4.2**
04BC004	68+97.5	6	3.5	74+67.5	6	3.3	**80+09.5**	**2.5**	**4**
04BC007	68+93	6'-6"	4.0"	74+53'-4"	6'-0"	4.25"	80+03	5'-2"	4.125"
04BC008	68+92	6'-0"	4.0"	74+52'-5"	5'-6"	4.25"	80+02	5'-2"	4.125"
04BC009	63+66	6'-0"	4.125"	69+27	6'-6"	4.125"	74+86	6'-0"	4.5"
04BC010	63+66	5'-0"	4.125"	69+27	5'-6"	4.0"	74+86	5'-0"	4.5"
04BC011	63+65	6'-0"	4.125"	69+26	6'-6"	4.0"	74+85'-6"	6'-0"	4.375"
04BC012	63+65	5'-0"	4.125"	69+26	5'-6"	4.0"	74+85'-6"	5'-0"	4.75"
04BC013	63+66	4'-6"	5.25"	69+27	5'-0"	4.625"	74+86	5'-0"	4.75"
04BC014	63+66	5'-6"	5.125"	69+27	6'-0"	4.75"	74+86	6'-0"	4.625"
04BC015	63+65	5'-0"	5.125"	69+26	5'-6"	4.75"	74+85	5'-6"	4.75"
04BC016	68+93	5'-6"	4.25"	74+59'-3"	5'-0"	4.5"	79+94	5'-0"	3.75"
04BC017	68+93	6'-6"	4.25"	74+59'-3"	6'-0"	4.5"	79+94	6'-0"	3.875"
04BC018	68+92	6'-0"	4.0"	74+58'-6"	5'-6"	4.5"	79+95	5'-6"	3.75"
04BC019	68+93	5'-6"	3.75"	74+53'-4"	5'-0"	4.125"	80+03	4'-4"	4.25"

The bold numbers at the top of the table represent the samples cored in the wheel path.
The last seven rows at the bottom of the table (shaded) represent the samples cored from the 102K lane.

The table shows that the thickness of the cores varies quite significantly taking into consideration that the design layer thickness was 4" (paved in two lifts). The values range from 3.1" for sample 3304BC002 to as high as 5.25" for sample 3304BC013, which makes the interpretation of the distresses observed in these cells very difficult. It is not clear if the buffer zones between the cells from where the samples were cored had less strict design requirements than the main area of the cells.

Out of the 17 cores received six were used for the fracture tests performed in this study. The three Superpave mixtures were designed to have the same aggregate gradation, with a nominal maximum aggregate size of 12.5-mm, an asphalt content of 5.8 percent, and air void content of 4 percent. The cores used and their volumetric properties are listed in Table 2.2.

Table 2.2. Volumetric Properties of the Field Cores

Mixture	Core #	G_{mm}	G_{mb}	Air Voids (%)
58-28 (Cell 33)	04BC003	2.501	2.356	5.8
	04BC004		2.355	5.8
	04BC007		2.357	5.8
	04BC011		2.342	6.4
	04BC016		2.344	6.3
	04BC017		2.330	6.8
58-34 (Cell 34)	**04BC001**	2.494	**2.343**	**6.1**
	04BC002		**2.337**	**6.3**
	04BC010		2.351	5.7
	04BC012		2.346	6.0
	04BC013		2.364	5.2
	04BC018		2.369	5.0
58-40 (Cell 35)	04BC002	2.491	2.327	6.6
	04BC008		2.353	5.5
	04BC011		2.362	5.2
	04BC013		2.331	6.4
	04BC014		2.324	6.7
	04BC017		2.339	6.1

The bold numbers represent the samples cored in the wheel path.
The shaded cells represent the samples cored from the 102K lane.

The air void values measured in the laboratory show significant differences in the air content of the different cores, with values ranging from 5.0% for sample 3404BC018 to 6.8% for sample 3304BC017, far above the design 4% value. Note that no significant differences are observed between the samples cored in the wheel path and the sample cored between the wheel path as well as the samples cored in the 80k lane versus the 102K lane.

In order to investigate the effect of the aging with depth, each core was cut into three 1" slices from top to bottom, and the remaining part was discarded. The slices were marked with T (Top), C (Center), and B (Bottom), respectively. The three plates were then cut into six semi circular bend (SCB) specimens with a diameter of 150mm and a nominal initial crack length of 15mm.

Considering the difference in the asphalt binders used in the three asphalt mixtures, different test temperatures were chosen for each mixture. The matrix of test temperatures for the three mixtures is shown in Table 2.3.

Table 2.3. Test Temperature Matrix

	Cell 33 (PG 58-28)	Cell 34 (PG 58-34)	Cell 35 (PG 58-40)
-18°C	X		
-24°C	X	X	X
-30°C	X	X	X
-36°C		X	X

Experimental Results

Six SCB specimens were machined out of each mixture core: two from the top (T), two from the center (C) and two from the bottom (B) slices. Two cores were tested at each of the three temperatures for each mixture, which results in 4 replicates per each mixture-position-temperature combinations with a total of 36 SCB specimens per mixture. For a few factor combinations only three replicate measurements were obtained.

The test data was then used to calculate the fracture toughness K_{IC} and fracture energy G_f according to the previously described methods. The means and coefficients of variation of both fracture parameters were calculated for each mixture at four different temperatures and shown in Table 2.4. The results are plotted in Figures 2.4 to 2.6.

Table 2.4. Average Fracture Properties for Each Mixture

Mixture	Temperature (°C)	Cores used	Fracture Toughness Mean (MPa.m$^{0.5}$)	CV*(%)	Fracture Energy Mean (N/m)	CV*(%)
58-28	-18	7, 17	0.762	7.7	311.09	17.9
	-24	3, 4	0.830	13.0	241.30	19.0
	-30	11, 16	0.804	8.6	243.82	26.0
58-34	-24	1, 2	0.894	14.9	353.77	23.0
	-30	10, 18	0.977	9.7	237.50	19.2
	-36	12, 13	0.929	7.8	266.55	18.2
58-40	-24	2, 13	0.776	14.4	345.95	12.8
	-30	14, 17	0.843	11.0	285.69	19.1
	-36	8, 11	0.920	12.1	274.68	17.0

*: Coefficient of Variation
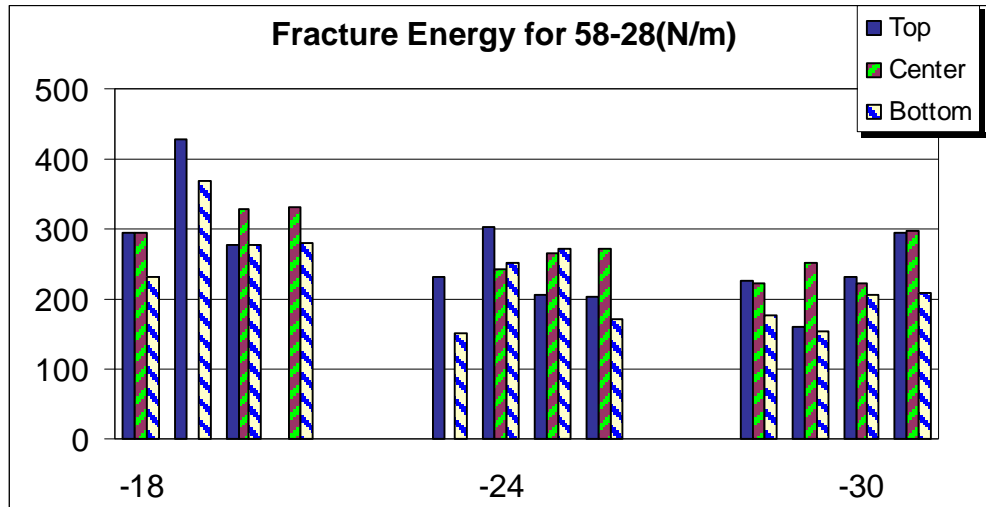
(a) Fracture Energy
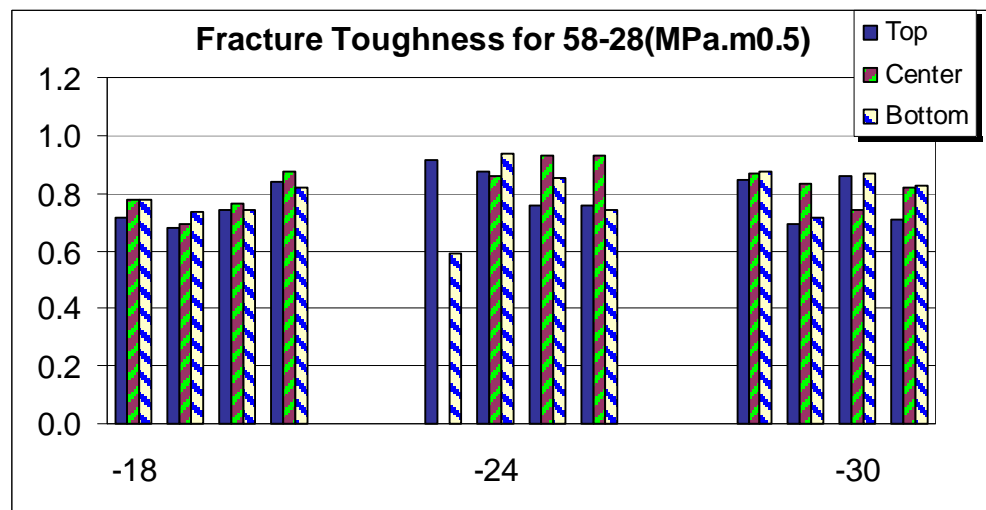
(b) Fracture Toughness

Figure 2.4. Testing Results for 58-28 Mixture
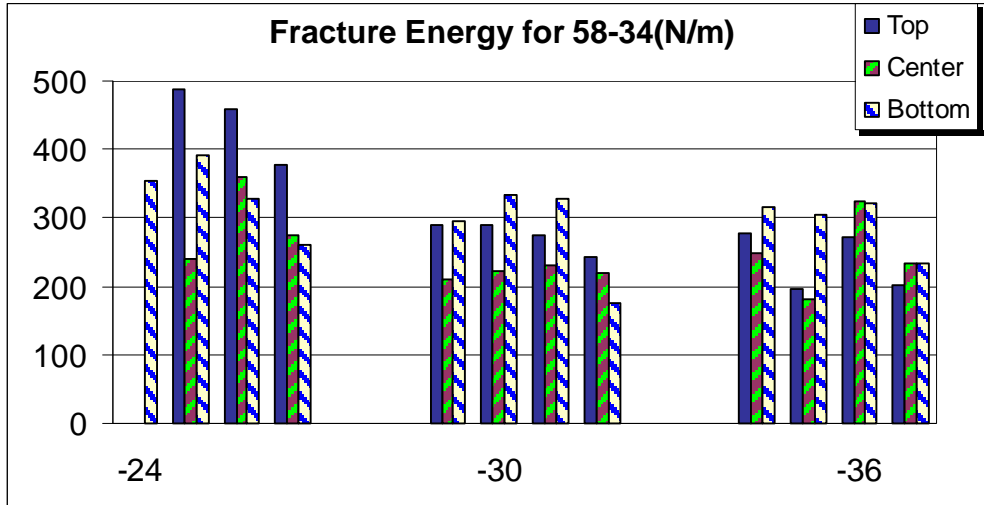
(a) Fracture Energy
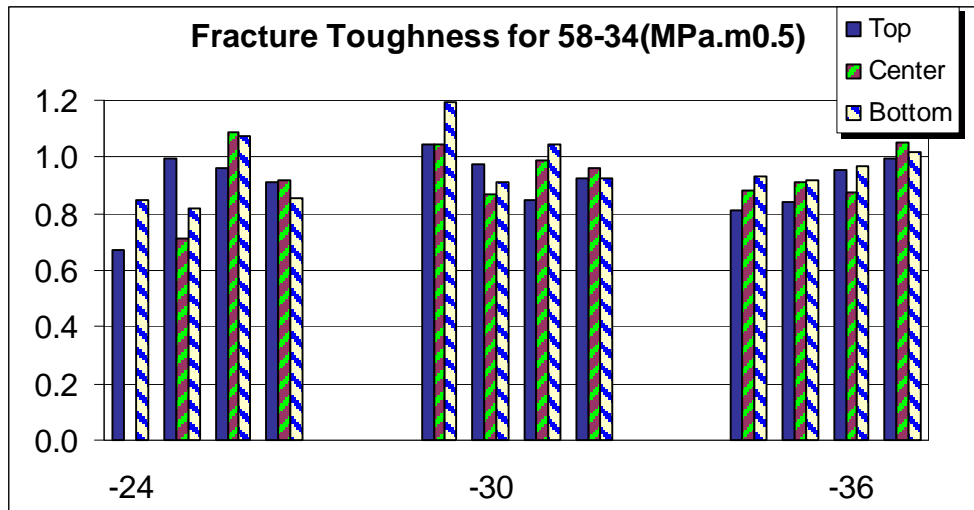
(b) Fracture Toughness

Figure 2.5. Testing Results for 58-34 Mixture
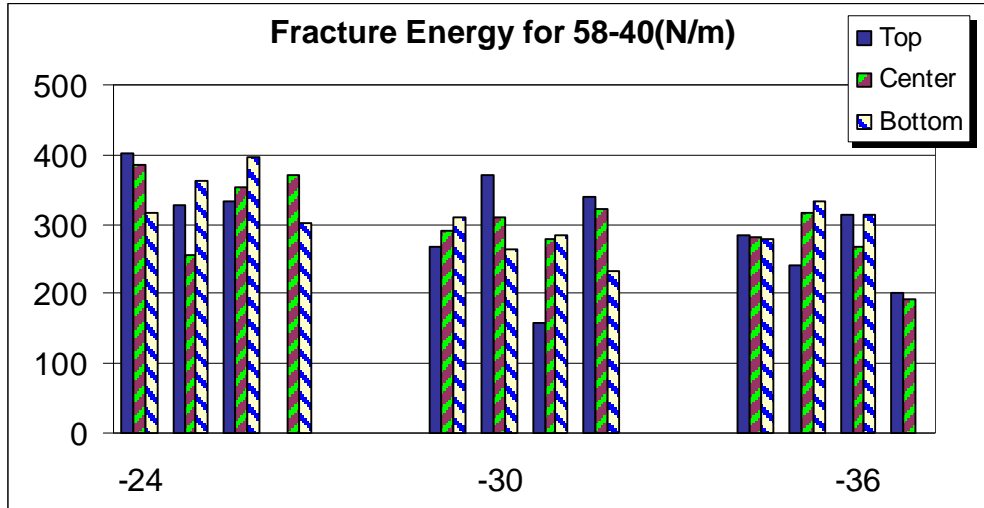
(a) Fracture Energy
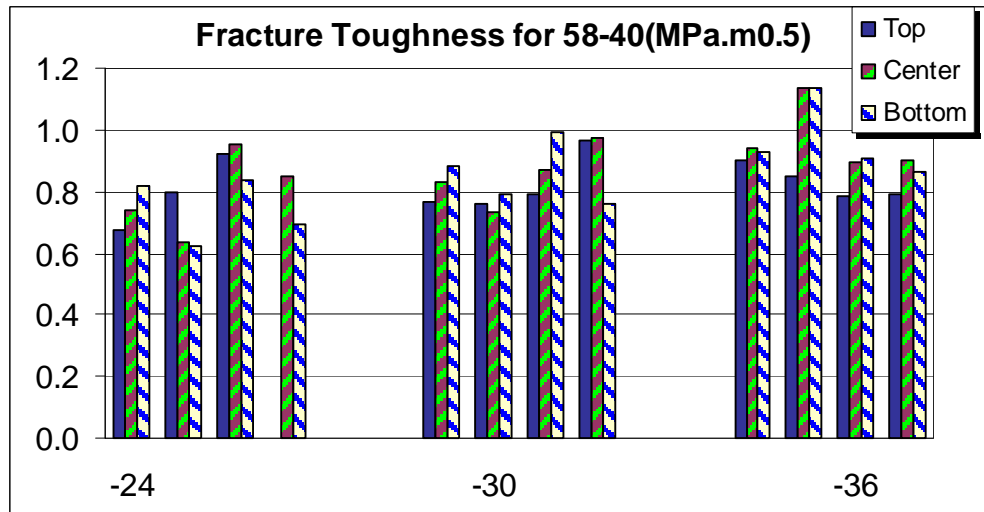
(b) Fracture Toughness

Figure 2.6. Testing Results for 58-40 Mixture

Analysis of Effects of Asphalt Binder, Temperature, and Layer

Three effects were tested in the statistical analysis: the type of asphalt binder (B), the temperature (T), and the layer effect related to aging (L). A split-plot analysis was used to examine the significance of these three factors. The type of asphalt binder and the temperature are the whole plot factors, and the layer effect is the split plot factor. The statistics software MacANOVA was used to perform the analysis. Only the two temperatures common for all three

mixtures, -24°C and -30°C, were used in the analysis. The p-values for K_{IC} and G_f are listed in Table 2.5.

Table 2.5. P-values from the analysis for three mixtures at -24°C and -30°C

Factors	Fracture Toughness (K_{IC})	Fracture Energy (G_f)
Temperature (T)	0.33685	0.00329
Binder (B)	0.067032	0.001568
B.T	0.51362	0.072562
Layer(L)	0.71053	0.11934
T.L	0.31478	0.4032
B.L	0.73018	0.016804
B.T.L	0.93612	0.33834

The factors corresponding to the p-values in the shadowed cells were significant. For the fracture toughness, the only significant factor is the type of asphalt binder; the main effect of temperature and the interaction between the temperature and the binder are not significant. This observation is different from the observation made in a previous study in which laboratory prepared specimens using the original loose mixtures from the same three cells were used; in that case none of the main effects of temperature and binder were significant, however, the interaction between them was significant (3).

For the fracture energy, both the temperature effect and the binder effect are significant, similar with the results obtained in the previous study. In addition, the interaction (B.L) between the layer effect and the binder effect is significant, which was not observed in the laboratory compacted specimens. This effect may result from the compaction in different lifts of the asphalt layer during construction or the potential material gradient introduced by the aging effect. Most likely, however, this is due to the increased variation in the field samples properties. The interaction (B.T) between the binder effect and the temperature effect is also marginally significant.

To better understand the main effects of binder, temperature, and layer and the interaction effects between them, interaction plots were used. The means of both fracture parameters were plotted against two factors in each of interaction plots, as shown in Figures 2.7 and 2.8. The values of the means are showed in both figures.
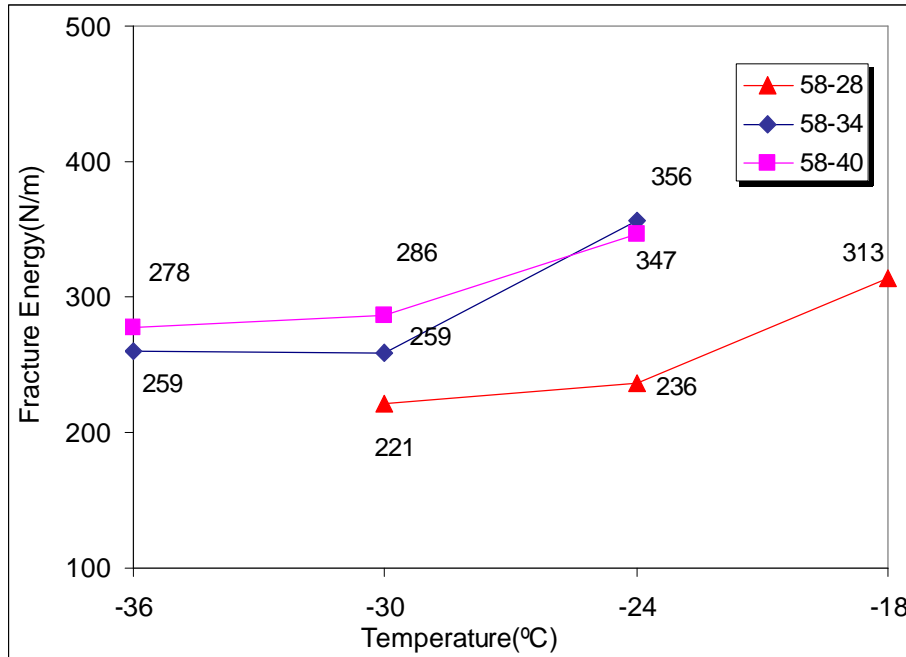
Figure 2.7. Fracture Energy versus Temperature by Binder
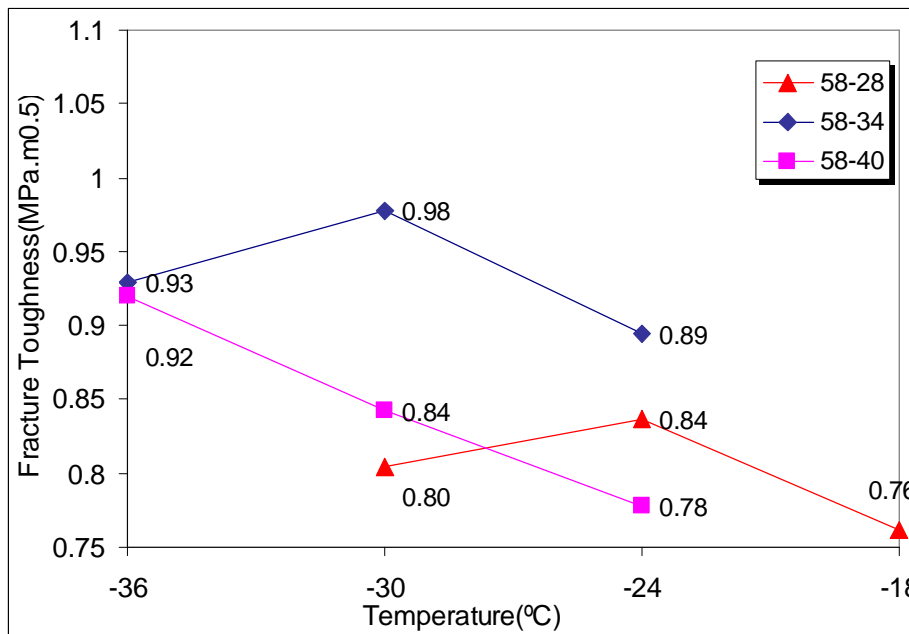
Figure 2.8. Fracture Toughness versus Temperature by Binder

In Figure 2.7, the three curves corresponding to the change in fracture energy with temperature of three asphalt mixtures are approximately parallel. This indicates the significant effect of the asphalt binder. Within the tested temperature range, the fracture energy increases as the temperature increases. As the temperature increases from -36°C to -30°C, the fracture energy

for the 58-40 mixture and the 58-34 mixture only shows minimal increase; as the temperature further increases to -24°C, both mixtures show significant increase; the 58-34 mixture changes at a faster rate than the 58-40 mixture such that the value of the fracture energy of the 58-34 mixture becomes larger than the 58-40 mixture energy at -24°C. A similar trend is observed for the 58-28 mixture shifted to warmer temperatures. These observations agree with those made in a previous study (4) and can be explained by the asymptotic behavior of asphalt mixtures at temperatures around and below the mixture glass transition temperature. As the temperature approaches the glass transition temperature, the mixture becomes brittle and less temperature dependent and the change in fracture energy levels off. This can also explain the marginal significance of the interaction effect (B.T) in the statistical analysis based on the data at -30°C and -24°C. Within this temperature range, the 58-40 mixture and the 58-34 mixture change rapidly, while the 58-28 mixture approaches its plateau of the change in properties. The higher values of fracture energy for the 58-40 mixture indicate that the use of a "softer" asphalt binder leads to an asphalt mixture with higher fracture energy given the same aggregate.

The change in fracture toughness shown in Figure 2.8 is more complex. The 58-34 mixture has the largest values of fracture toughness and ranked highest for all three temperatures. This is different from the ranking by fracture energy. Both the 58-34 mixture and the 58-28 mixture show the existence of a peak value; the 58-40 mixture, however, monotonically decreases as the temperature increases. In the previous study in which laboratory prepared SCB specimens were used the peak fracture toughness values were explained by two opposite actions occurring in asphalt mixtures: the strengthening grip from of the asphalt matrix and the micro damage due to thermal shrinkage. The temperature at which the peak value of fracture toughness is reached was predicted to be around the PG lower limit temperature of asphalt binder (4). This prediction seems to hold for the 58-34 mixture and the 58-28 mixture: the peak value of fracture toughness is reached around -30°C for the 58-34 mixture, and around -24°C for the 58-28 mixture. For the 58-40 mixture, the test temperatures used were most likely not low enough to detect the peak fracture toughness

Analysis of the Aging Effect

The results obtained in this study and the results obtained in a previous study on laboratory prepared SCB specimens were compared in this section to investigate the significance

of the aging effect on the fracture properties of asphalt mixtures. The field samples were tested at -24°C, -30°C, and -36°C for the 58-34 mixture and the 58-40 mixture, and at -18°C, -24°C, and -30°C for the 58-28 mixture to match the test temperatures used in the asphalt binder investigation. The laboratory prepared specimens were tested at three temperatures: -20°C -30°C, and -40°C.

The interaction plot for fracture energy plots the means of fracture energy against the temperature by the type of binder. Figure 2.9 reproduces the results obtained on the laboratory prepared specimens. Figure 2.10 contains the results from both studies.
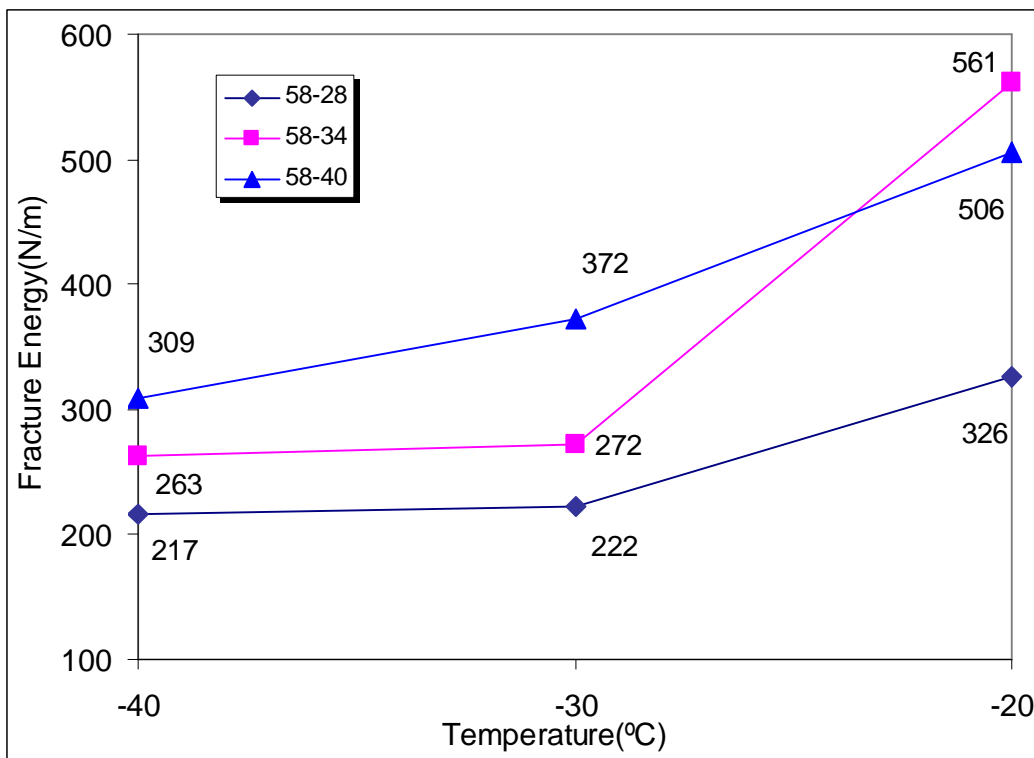
Figure 2.9. Interaction Plot of G_f for Laboratory Prepared Specimens
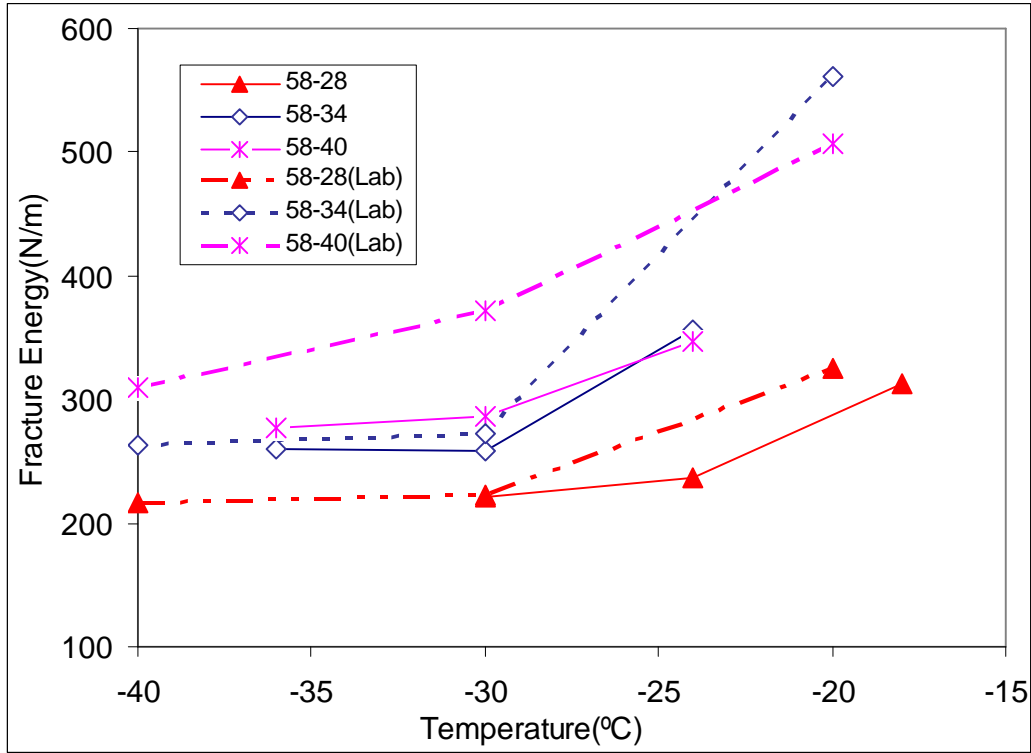
Figure 2.10. Interaction Plot of G_f for Both Lab-compacted and Field Specimens

The evolutions of fracture energy of the laboratory prepared specimens and of the field samples have considerable similarities. The laboratory specimens and the field samples energy curves are almost parallel for all three mixtures. For all mixtures the field samples have lower fracture energy than the laboratory prepared specimen and they were less temperature susceptible. This may be explained by the aging that occurred in the field samples which most likely made these materials more brittle than the laboratory specimens. This comparison clearly indicates that the fracture energy of the mixtures diminishes with service life which results in less fracture resistance of the mixtures. The highest reduction is observed for the 58-40 mixture and the lowest for the 58-28 mixture.

The interaction plots for fracture toughness are shown in Figure 2.11 and 2.12. Figure 2.11 reproduces the results obtained for the laboratory prepared specimens. Figure 2.12 contains the results from both studies.

32
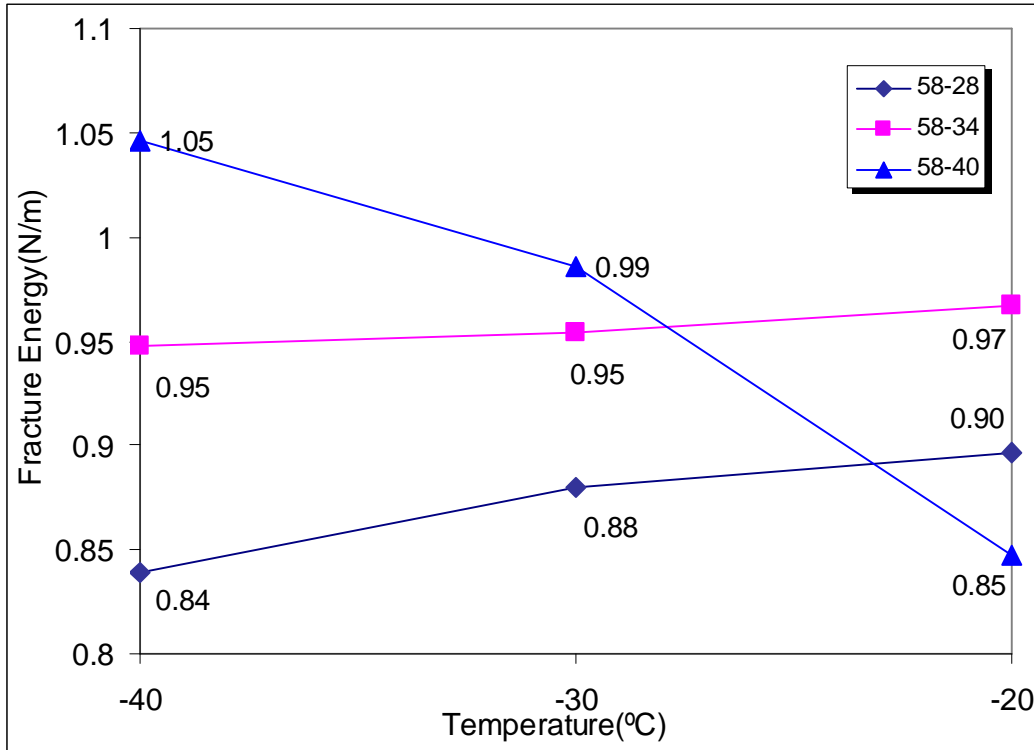
Figure 2.11. Interaction Plot of K_{Ic} for Lab-compacted Specimens
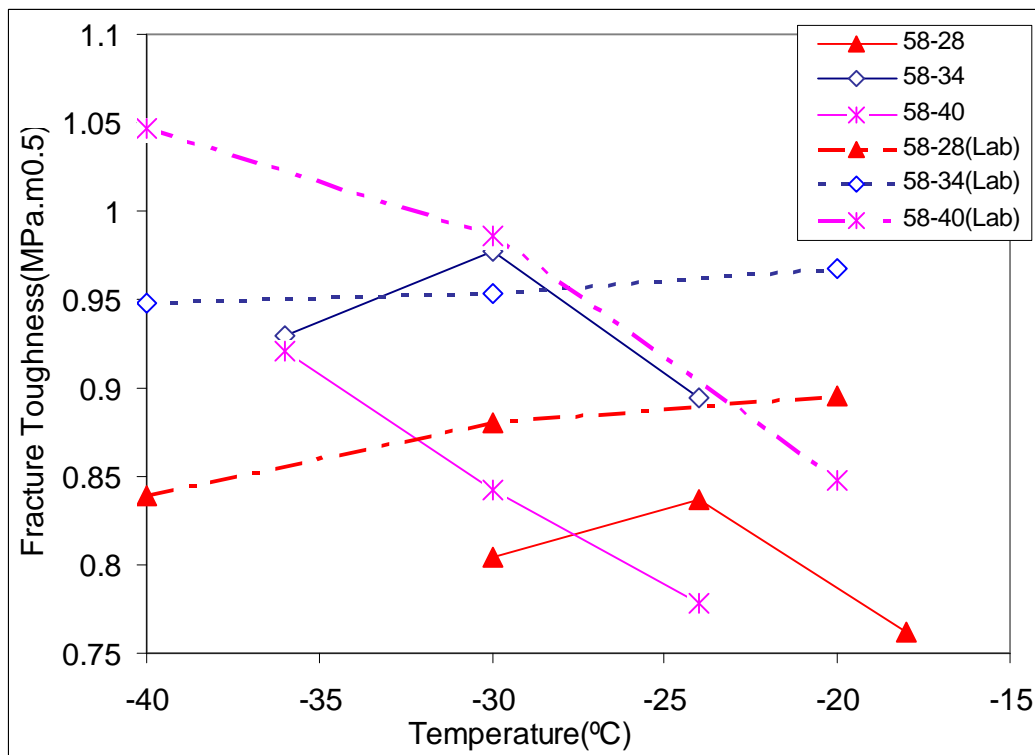
Figure 2.12. Interaction Plot of K_{Ic} for Both Lab-compacted and Field Specimens

With the exception of the results for the 58-34 mixture at -30°C (0.98 $MPa \cdot \sqrt{m}$ for the field samples compared to 0.95 $MPa \cdot \sqrt{m}$ for the laboratory specimens) the fracture toughness of the laboratory specimens is larger than the fracture toughness of the field samples. Both the 58-34 mixture and the 58-28 mixture show the existence of a peak value of fracture toughness as the temperature drops from above the PG limit to below the PG limit. For the 58-40 mixture the test temperatures were most likely not low enough to reach the toughness peak value.

Both the fracture toughness and fracture energy results indicate that the field samples have lower fracture resistance than the laboratory specimens. A statistical analysis was performed to confirm this observation using the results obtained at -30°C. Two factors were analyzed: the type of asphalt binder (B) with three levels and the effect of degradation in the field with two levels (Age). The field degradation may result from other factors, such as accumulation of the traffic loading in addition to aging. The layer effect was not considered in this analysis. A factorial analysis was performed and the p-values are listed in Table 2.6. The small p-values for the aging effect for both fracture parameters show that the laboratory specimens are statistically significant different from the field samples in terms of both the fracture toughness and the fracture energy. Note that the p-values for the interaction between the binder effect and the aging effect were also small which indicates that under similar conditions different asphalt mixtures age differently.

Table 2.6. P-values for the Field Degradation Analysis

Factors	Fracture Toughness (K_{IC})	Fracture Energy (G_f)
Aging (Age)	0.0013	0.0137
Binder (B)	5.6e-06	1.6e-07
Age.B	0.098	0.054

It should be mentioned that another factor may have contributed to the difference in properties: the air void content difference between the field samples and the laboratory compacted specimens. These values are listed in Table 2.7. The difference in air void content between the field and laboratory specimens varies from 1.3% for 58-28 mixture to 2.2% for 58-34 mixture. The contribution of the air void content to the fracture resistance of asphalt mixtures needs to be examined in future research. Previous research performed on limited numbers of specimens has

indicated a reduction in the fracture resistance of the asphalt mixtures with an increase in air void content.

Table 2.7. Air Voids Contents for Three Mixtures

Type of Mixture	Specimen Conditioning	Specimen ID.	Air Voids (%)	Average
58-28	Laboratory Specimen	28-4	4.9	5.0
		28-5	5.0	
	Field Sample	33-11	6.4	6.3
		33-16	6.3	
58-34	Laboratory Specimen	34-5	3.4	3.2
		34-6	3.0	
	Field Sample	34-10	5.7	5.4
		34-18	5.0	
58-40	Laboratory Specimen	40-5	4.7	4.5
		40-6	4.2	
	Field Sample	35-17	6.1	6.4
		35-14	6.7	

Summary and Conclusions

Field samples cored from cells 33, 34, and 35 from the MnROAD facility were tested using the SCB test. The fracture toughness and fracture energy were obtained and statistical analysis was performed to identify the significance of the following factors: type of asphalt binder, temperature, and the aging effect along the depth of the asphalt pavement. In addition, the fracture properties of the field samples were compared to the fracture properties of laboratory prepared specimens using loose mix from the same cells collected at the time of construction of the cells.

A number of conclusions were drawn in this task:

1. The fracture energy of the field samples is significantly affected by the temperature and the type of binder used.

2. The fracture toughness of the field samples is significantly affected by the type of binder used.

3. The evolutions of the fracture toughness and fracture energy with type of binder and temperature are similar for the field samples and laboratory specimens.

4. The field samples and the laboratory specimens are statistically different with respect to both the fracture toughness and the fracture energy:

- The fracture energy of the field samples is lower than the fracture energy of the laboratory specimens.

- The fracture toughness of the field samples is lower than the fracture energy of the laboratory specimens with the exception of the 58-34 mixture at -30°C.

- Statistical analysis shows that the interaction effect between the asphalt binder and the aging effect is significant which indicates that the three asphalt binders used in this study age differently.

CHAPTER 3

Asphalt Binder Testing

Introduction

One of the factors that significantly affects the performance of asphalt pavements during their service life is the aging of the asphalt binder used in the construction of the pavement. In particular, the aging process negatively affects the fracture resistance of the asphalt mixtures against low temperature cracking and thermal and traffic induced fatigue cracking. In spite of the considerable advancements made in the past years in understanding the evolution of the aging process and in simulating field aging in laboratory conditions for material specification purposes, there are a number of critical issues that are still not well understood. Among them, the issue of the pavement depth at which aging effects become less significant and the issue of the reasonableness of the laboratory aging methods to simulate field aging, in particular for polymer modified binders, are generating a strong debate in the research community.

Objectives

In the previous task, the fracture properties of asphalt mixtures used in the construction of the MnROAD facility were investigated. Field cores were taken from the cells and 1″ test samples were cut and tested using the semi circular bend (SCB) test to determine the fracture properties of the field mixtures and to evaluate the effect of aging with depth. The tested samples were then used to extract and recover the binders used in their preparation for further investigation.

This task presents the results of this investigation. The rheological properties of the binders extracted and recovered from the three MnROAD cells are compared with the properties of the original binders aged in laboratory conditions, and the effect of the sample location within the pavement on the rheological properties of the extracted binders is evaluated.

Materials

The three binders studied in this paper were obtained from MnRoad cells 33, 34 and 35. The cores were taken from MnROAD approximately 5 years after the construction of the cells. Three

asphalt binders in the mixtures are: PG 58-28 for cell 33, 58-34 for cell 34, and 58-40 for cell 35. The design layer thickness was 4" and the layer was paved in two lifts.

The 150mm diameter samples were cored directly from MnRoad through the full depth of the HMA layer. The cores were cut off the bottom to a final height of around 100mm. In order to investigate the effect of the aging with depth, the cores were cut into three 1" slices from top to bottom, and the remaining part was discarded. The slices were marked with T (Top), M (Middle), and B (Bottom), respectively. After the mixture testing was performed, the asphalt binders were extracted from the cores according to MN/DOT Modified AASHTO T164 method (5). This method uses toluene as extraction solvent to prevent any interaction with the polymer present in the 58-34 and 58-40 binders, as suggested in SHRP A-370 (6). Several cores were combined for each mixture to extract enough binder to perform the binder tests. Nine binders were recovered from the sliced cores as shown in Table 3.1. It is interesting to note that the field samples contained less binder than the 5.8 percent design value; the difference was particularly significant for the polymer modified PG 58-40 binder.

Table 3.1. Recovered Asphalt Binders

Sample Name	Cell	Original Binder Grade	Location in Core	Binder Content (%)
33T	33	PG58-28	Top layer	5.78
33M	33	PG58-28	Middle layer	5.52
33B	33	PG58-28	Bottom layer	5.65
34T	34	PG58-34	Top layer	5.76
34M	34	PG58-34	Middle layer	5.47
34B	34	PG58-34	Bottom layer	5.13
35T	35	PG58-40	Top layer	4.84
35M	35	PG58-40	Middle layer	5.04
35B	35	PG58-40	Bottom layer	5.06

In addition to the extracted binders, the three original binders used in the construction of the three cells were aged in the laboratory using the RTFOT and PAV methods (7, 8).

Experimental Procedure

The dynamic shear rheometer (DSR) testing was performed on a TA AR 2000 rheometer, according to AASHTO T 315 (9). However, for master curve generation purposes frequency

sweeps from 1 to 100 rad/s were performed over a temperature range from 4°C to 76°C. At lower temperatures (4° to 34°C) the tests were performed on 8-mm plates with a 2.0 mm gap. At high temperatures (34° to 76°C) the tests were performed on 25-mm plates with a 1.0 mm gap.

The bending beam rheometer (BBR) testing was performed on a Cannon thermoelectric rheometer, according to AASHTO T 313 (10). Tests were performed at two temperatures. For the extracted binders testing was performed at higher temperatures than the original PG grade called for. For example, a PG 58-28 binder was tested at -12°C and -18°C instead of -18°C and -24°C.

Direct tension (DT) testing was carried out on a Bohlin Direct Tension with Neslab chilling system, according to AASHTO T 314-02 (11). The binders were tested at the same test temperatures as the BBR tests.

In addition, the DT procedure was modified to perform Double Edge Notch Tension (DENT) tests based on previous work performed by Gauthier and Anderson (12). The DT molds were modified to prepare DENT test specimens according to the geometry shown in Figure 3.1. The modified molds also allowed the use of a razor blade to generate 1.5mm pre-cracks on both sides of the test specimens. The strain rate was lowered to 1.8%/min due to the rapid failure occurring at the lower temperature.
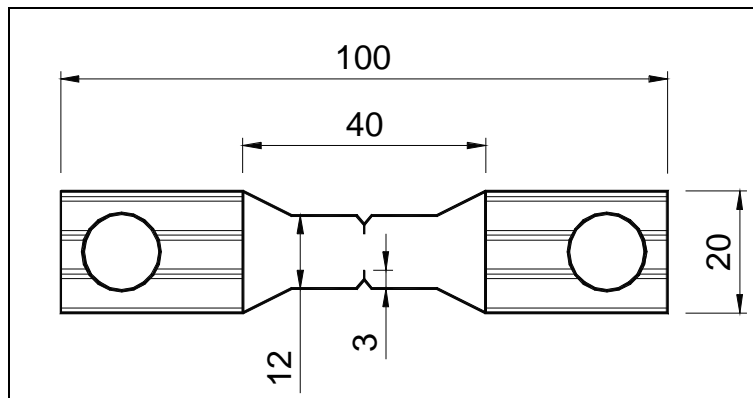
Figure 3.1. Double Edge Notched Tension (DENT) specimen dimensions (mm)

Experimental Data Analysis

The experimental data obtained for the original binders aged in laboratory conditions and for the extracted and recovered binders from the filed cores was used to investigate the effect of aging on the properties of these binders. The change in properties at high and low service temperatures was investigated by calculating limiting temperatures based on the current PG

specifications, as well as on the new fracture test previously mentioned. In addition, complex modulus and phase angle master curves were generated to investigate the change in behavior over a wider range of frequencies and temperatures.

High Temperature

The DSR data obtained at 10rad/s was used to determine the limiting temperature at which $|G^*|/\sin\delta$ (the absolute value of the complex modulus divided by the sin of the phase angle) equals 2.2 kPa. A number of observations can be made based on the results presented in Table 3.2.

Table 3.2. Temperature Values at which $|G^*|/\sin$ d = 2.2kPa, °C

Cell	Condition				
	RTFOT	**PAV**	**Extracted Top**	**Extracted Middle**	**Extracted Bottom**
33	63.4	72.7	75.1	72.6	73.1
34	63.9	73.4	72.2	70.1	70.0
35	66.1	76.5	74.0	68.9	68.5

For all three cells, the top layer has higher limiting temperatures than the other two layers, which indicates that more aging occurred in this layer. This is in particular true for the PG -40 binder for which the differences were as high as 5.5°C. The differences between the middle and the bottom layers were not significant.

With respect to laboratory versus field aging, the results indicate that for cell 33 the three extracted binders were stiffer than the PAV-aged binder. However, for cells 34 and 35 the extracted binders were softer than the PAV-aged binder. This was more pronounced for cell 35 binder. It is not clear if this trend is related to the presence of modifiers in the PG -34 and -40 binders.

DSR Master Curves

The frequency sweep data from the DSR testing was used to obtain master curves of the complex modulus and phase angle, as shown in Figures 3.2 to 3.7. For comparison purposes all master curves were obtained at a reference temperature of 34ºC. A commercial computer program was used to fit the Christensen-Anderson-Marasteanu (CAM) model to the $|G^*|$ test data (13):

$$\left|G^{*}(w)\right| = G_{g}\left[1+\left(\frac{W_{c}}{w}\right)^{v}\right]^{-\frac{w}{v}} \tag{3.1}$$

where

$|G^{*}(w)|$ = absolute value of complex modulus as a function of frequency w (GPa)

G_{g} = glassy modulus

W_{c}, v, w = model parameters

The shift factors were determined simultaneously with the coefficients of the model and were also used to generate phase angle master curves.

The |G*| master curves shown in Figures 3.2 to 3.4 indicate that binders extracted from cells 33 and 34 have approximately the same stiffness as the PAV-aged binder, and that was very little difference between the three layers cut from the cores. However, for cell 35 the top layer was significantly stiffer than the middle and bottom layers and the recovered binders were all stiffer than the PAV-aged binder. In addition, the master curves had different slopes, indicating different temperature susceptibilities between field and laboratory-aged binders.

The most significant differences between field and laboratory-aged binders are noticed in the phase angle master curves shown in Figures 3.5 to 3.7. For the unmodified binder in cell 33, the differences were minimal. However, for the modified binders in cells 34 and 35 the plateau seen in the PAV-aged binders disappears for the recovered binders. This seems to indicate that the polymer effect is not present in the recovered binders; it is not clear if this is a result of the extraction process or of the field aging mechanism. For this two binders the top layer had noticeable lower phase angle values than the middle and bottom layers, possibly indicating higher aging of the binder in the top layer.
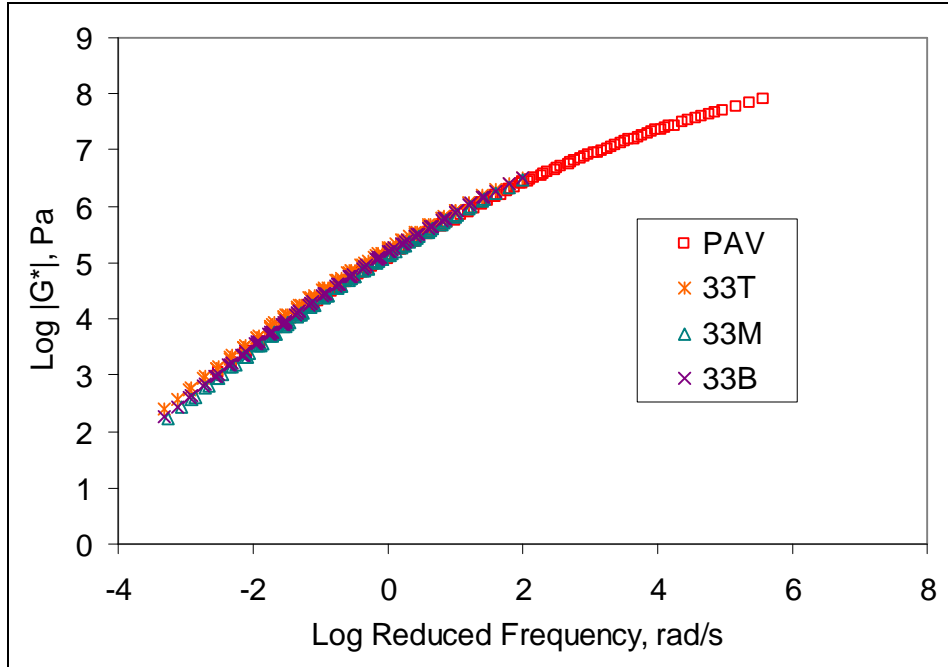
Figure 3.2. Complex modulus master curve – Cell 33, T_{ref} = 34°C
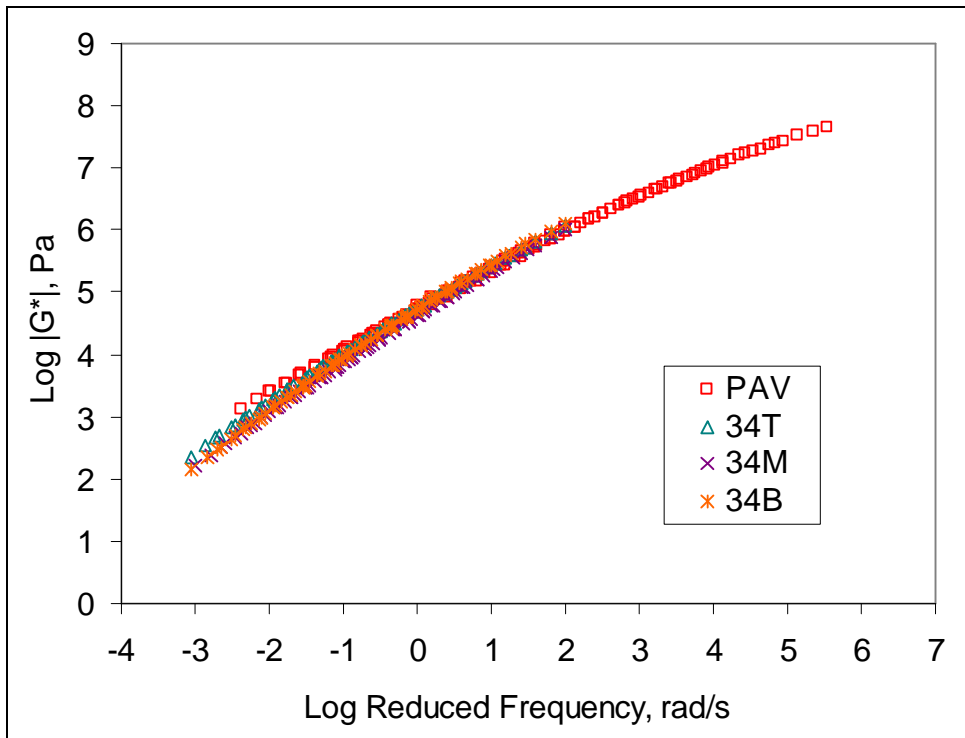
Figure 3.3. Complex modulus master curve – Cell 34, T_{ref} = 34°C
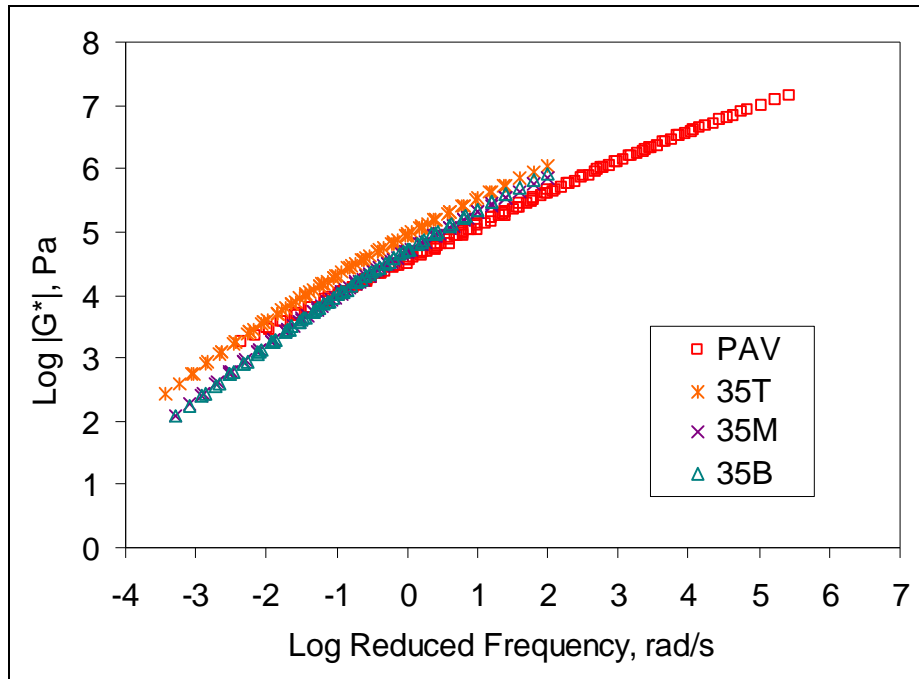
Figure 3.4. Complex modulus master curve – Cell 35, $T_{ref} = 34°C$
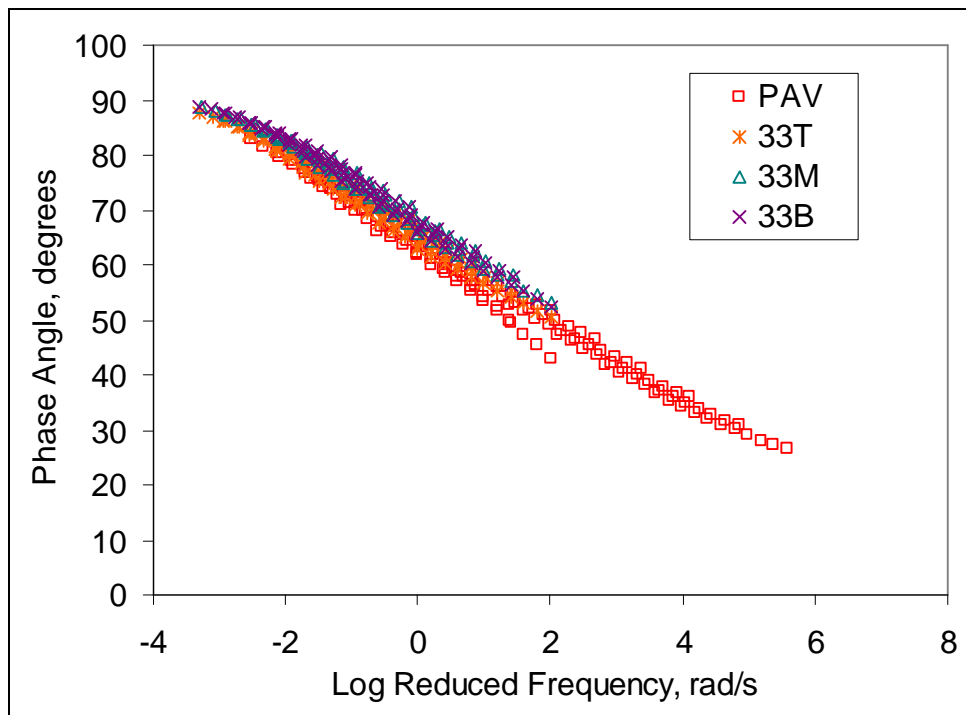
Figure 3.5. Phase angle master curve – Cell 33, $T_{ref} = 34°C$
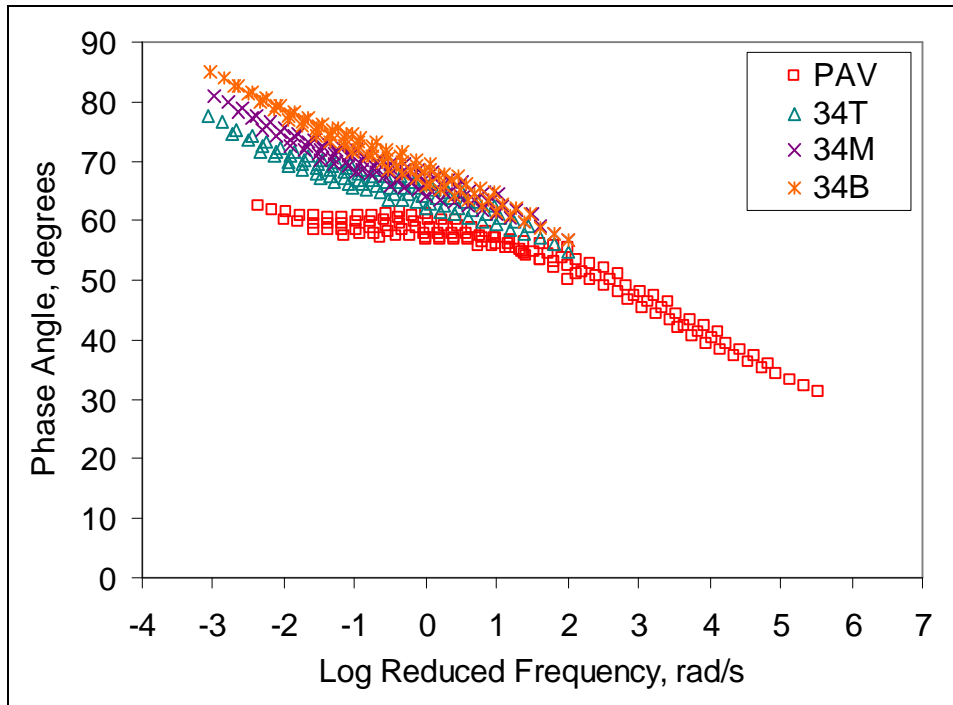
Figure 3.6. Phase angle master curve – Cell 34, T$_{ref}$ = 34°C
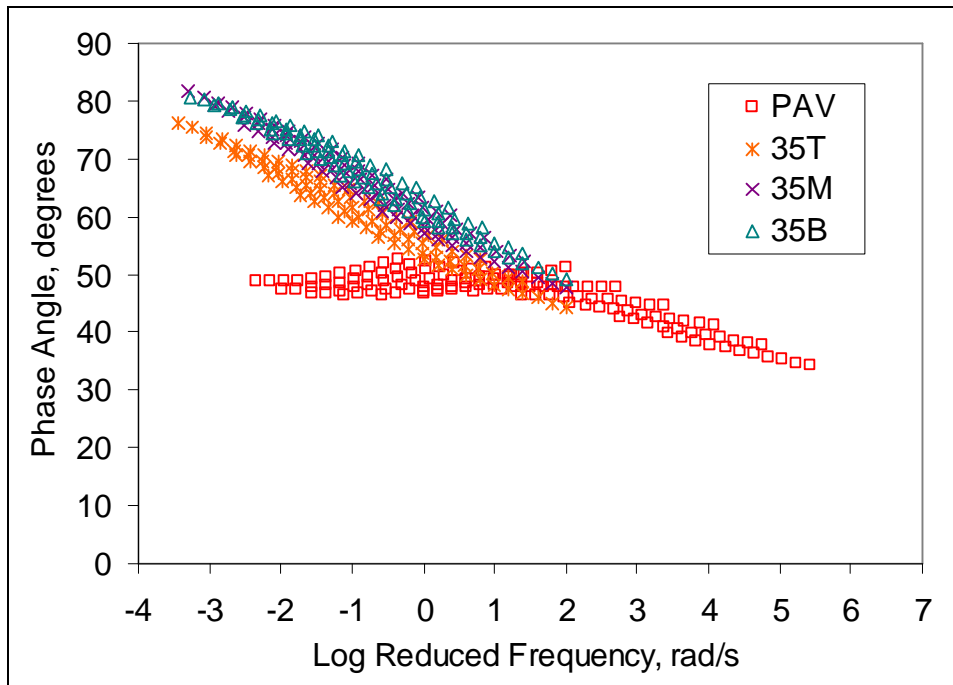
Figure 3.7. Phase angle master curve – Cell 35, T$_{ref}$ = 34°C

Low Temperature

The BBR, DTT and DENT data was used to determine various limiting temperatures that can be used to investigate the low temperature behavior of the binders at low temperatures. The results are shown in Table 3.3. Note that the table includes several critical temperatures based on variations from the current MP1a specification (14). The second to last column contains the critical temperature values determined using the BBR data only based on a method proposed by Shenoy (15). The critical temperature represents the intersection of the asymptote to the thermal stress curve at -40°C with the horizontal temperature axis. The last column contains the critical temperatures obtained by intersecting the binder thermal stress without any adjustment (the pavement constant PC = 1) and the strength master curve obtained from the DENT data. This approach was used as a consequence of the observation that the strength values for the pre-cracked DENT specimens were 3 to 5 times lower than the strength values measured using the current DTT procedure.

Table 3.3. Critical Low Temperature Values from Different Failure Criteria, °C

| Binder | BBR | | DTT | T_{cr} (PC=18) | | T_{cr} (PC=1) |
	S(60s)= 300MPa	m(60s)= 0.300	$\varepsilon_{failure}$= 1%	BBR and DTT	BBR	BBR and DENT
Cell-33-T	-28.7	-25.8	-31.5	-29.7	-30.5	< - 40
Cell-33-M	-29.1	-26.1	-29.3	-25.9	-30.7	-33.9
Cell-33-B	-28.3	-25.8	-31.6	-30.6	-30.7	-35.5
33PAV	-30.9	-29.8	-26.2	-28.2	-31.8	-34.1
Cell-34-T	-33.4	-30.7	-41.1	-37.4	-31.8	< -40
Cell-34-M	-32.9	-30.8	-41.2	-36.4	-32.0	-34.3
Cell-34-B	-32.5	-29.4	-39.4	-33.8	-31.7	-37.2
34PAV	-35.1	-35.5	-34.7	-35.3	-32.1	< -40
Cell-35-T	-41.0	-28.6			-32.0	
Cell-35-M	-42.3	-29.4	-44.9	< -40	-31.5	< -40
Cell-35-B	-43.0	-31.6	-45.7	< - 40	-30.1	< -40
35PAV	-45.8	-43.8	-48.0	< -40	-33.1	< -40

The stiffness and m-value limiting temperatures for all three cells were lower for the PAV aged binders than the recovered binders, which may indicate more aging in the field binders. For stiffness, the differences are relatively small with the exception of the PG -40 binder for which the difference was as high as 4.8°C. The differences between the different layers

binders were not very significant, with the exception of the PG -40 binder for which the differences were as high as 2°C between the top and the bottom layer. However, the most significant change is observed in the m-value limiting temperatures of the recovered binders compared to the PAV values. For the PG -40 binder the change was as high as 15.2°C, which clearly indicates a significant change in the relaxation properties of the recovered binder compared to the laboratory aged binder in spite of the less significant change in stiffness.

The DTT limiting temperatures based on the failure strain criterion were noticeably higher for the PAV-aged binders compared to the recovered one, with the exception of the PG -40 binder for which the opposite was observed. The DTT limiting temperatures were relatively similar to the BBR stiffness limiting temperatures for the PG -28 and -40. The DDT values were significantly lower (almost 8°C) compared to the BBR values for the PG -34 binder.

The T_{cr} values obtained using the current MP1a method were relatively similar to the BBR stiffness limiting temperatures, with the exception of the PG -34 binder for which the temperatures were significantly lower, as observed for the DTT values. The T_{cr} values obtained only from the BBR data matched relatively well the BBR stiffness limiting temperatures, with the exception of the PG -40 binder for which the values were almost 10°C higher than the BBR temperatures. It is interesting to note that the T_{cr} calculated from the BBR creep data and the DENT strength data matched reasonably well in some cases the BBR and DTT limiting temperatures without the use of the binder–mixture conversion factor, the so called pavement constant.

In addition to the limiting temperatures comparison, a direct comparison of the BBR stiffness curves for the three extracted binders and the PAV-aged binder was performed for each cell, as shown in Figures 3.8 to 3.10. The comparison confirms the trend observed in the limiting temperature analysis that for all three cells the extracted binders were always stiffer than the PAV-aged binders. The figures also show the significant reduction in the slope of the stiffness curves for the recovered binders compared to the PAV-aged binder. With respect to the different layers the differences in stiffness are relatively small and follow the expected trend of a stiffer top layer compared to the middle and bottom layers only for the PG -40 binder.
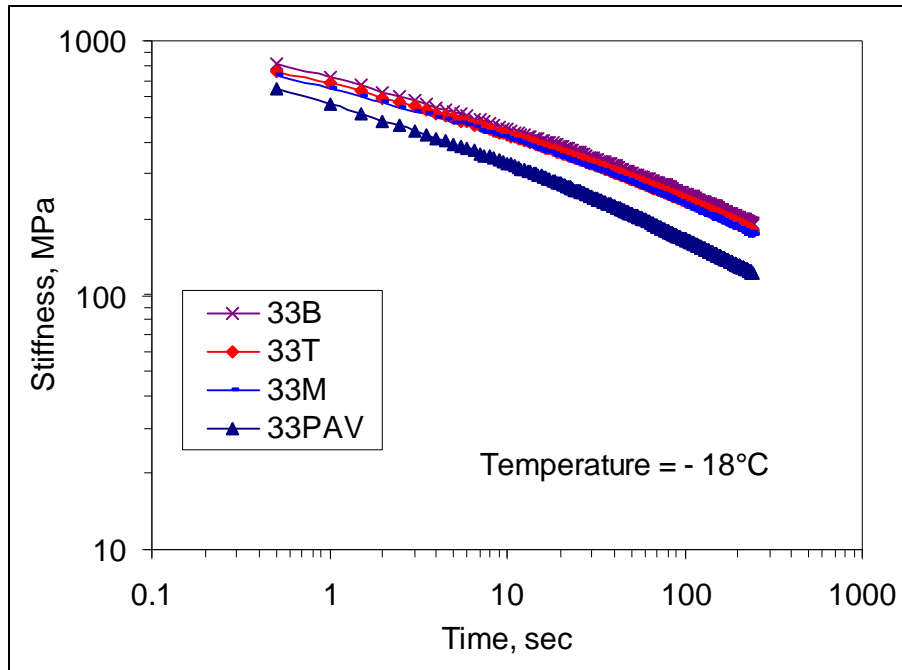
Figure 3.8. BBR stiffness comparisons, Cell 33
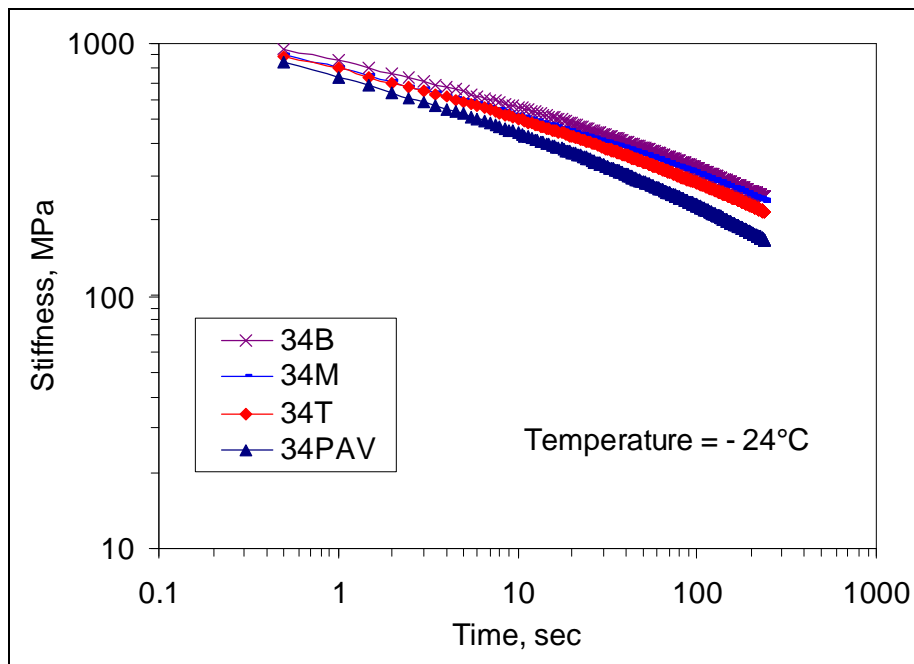
Figure 3.9. BBR stiffness comparisons, Cell 34
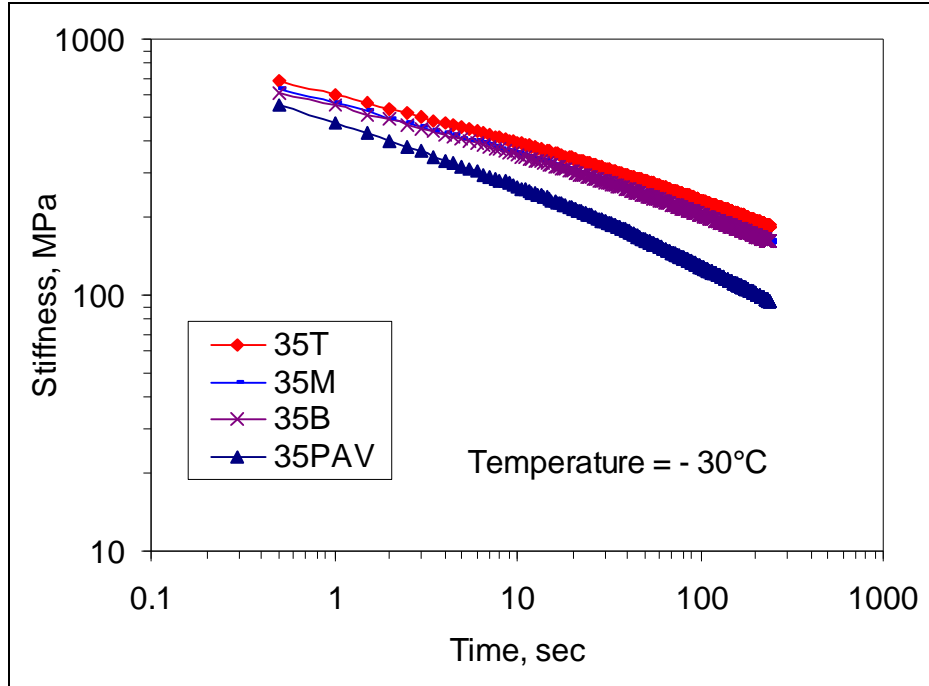
Figure 3.10. BBR stiffness comparisons, Cell 35

Fracture Toughness

The data obtained using the DENT testing procedure described previously was used to calculate the fracture toughness K_{IC} based on the following equation (16):

$$K_{IC} = \frac{P}{B\sqrt{W}} f(a/W)$$

$$f(a/W) = \frac{\sqrt{\dfrac{pa}{2W}}}{\sqrt{1 - \dfrac{a}{W}}}\left[1.122 - 0.561\left(\frac{a}{W}\right) - 0.205\left(\frac{a}{W}\right)^2 + 0.471\left(\frac{a}{W}\right)^3 + 0.190\left(\frac{a}{W}\right)^4\right] \quad \textbf{(3.1)}$$

where

      P - peak load

      B - specimen thickness (equal to 6mm)

      W - half width of the specimen (equal to 6mm)

      a – notch width (equal to 3mm)

      A comparison of the fracture toughness values for the PAV-aged and the recovered binders is shown in Figure 3.11 to 3.13. Figure 3.11 indicates that for cell 33 there are no

significant differences between the binders recovered from the different layers and between the recovered binders and the PAV-aged binder.
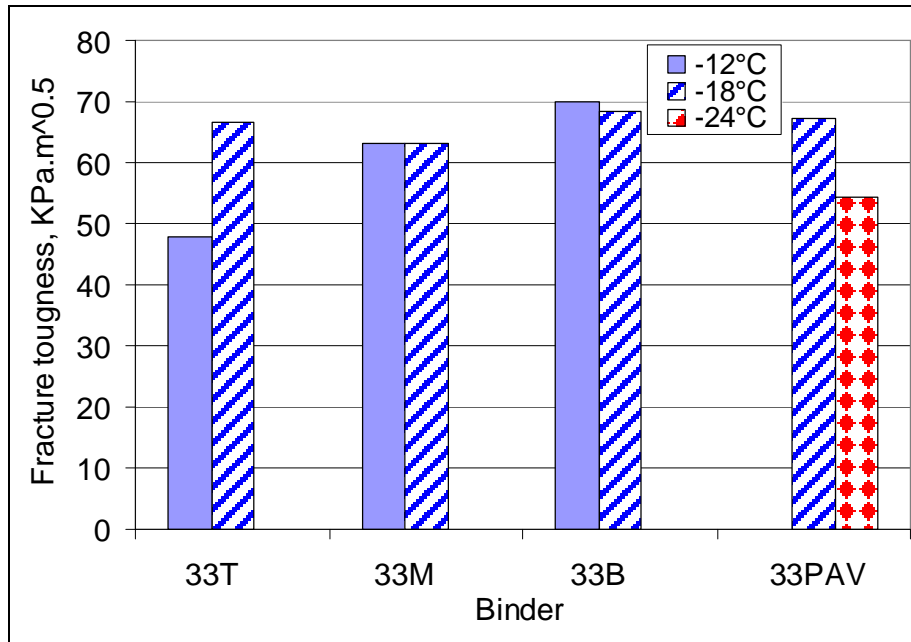
Figure 3.11. Fracture Toughness for Cell 33 Binders

Figure 3.12 clearly indicates that for cell 34 the PAV-aged binder has a higher toughness than the recovered binders at -24°C. No clear trend is observed for the change in toughness with layer location.
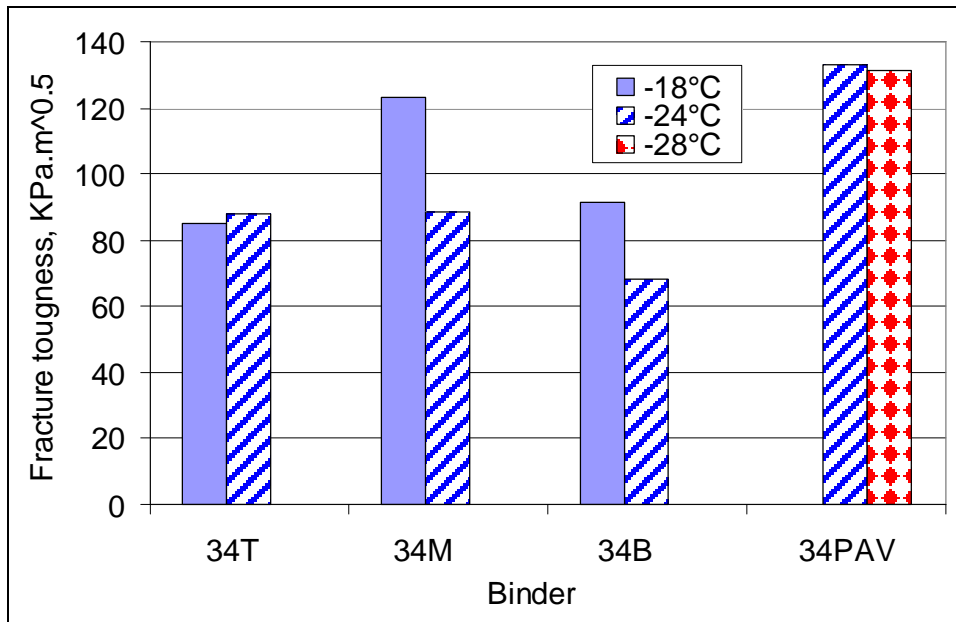
Figure 3.12. Fracture Toughness for Cell 34 Binders

Figure 3.13 shows that for cell 35 the PAV-aged binder also has a higher K_{IC} value than the recovered binders; however, the top layer has a lower K_{IC} value than the middle layer, which in turn is lower than the bottom layer value, which may indicate higher aging effects in the top layer. It is important to note that the K_{IC} values at -24°C for the top layer of cell 34 and cell 35 are very similar, which indicates similar fracture resistance in spite of the different grade of the original binders.
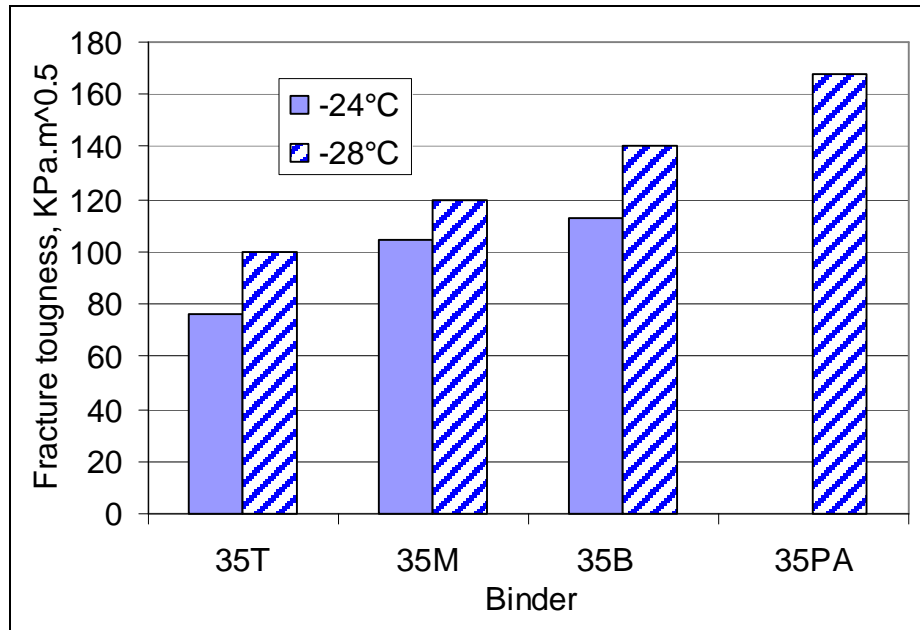
Figure 3.13. Fracture Toughness for Cell 35 Binders

Summary and Conclusions

The properties of three binders recovered from cores taken out of MnRoad cells 33, 34 and 35 were analyzed in this task. In addition to the recovered binders, the laboratory-aged original binders used in the construction of the three cells were also investigated. In order to investigate the effect of the aging with depth, the cores were cut into three 1" slices from top to bottom, and the remaining part was discarded.

The experimental data was used to investigate the effect of aging on the properties of these binders by calculating limiting temperatures based on the current PG specifications, as well as on a new fracture test. In addition, complex modulus and phase angle master curves were generated to investigate the change in behavior over a wider range of frequencies and temperatures.

The high temperature DSR data showed that for all three cells the top layer had higher limiting temperatures than the other two layers, in particular for the PG -40 binder for which the difference top to bottom was as high as 5.5°C. The differences between the middle and the bottom layers were not significant. With respect to laboratory versus field aging, the results indicate that for cell 33 the three extracted binders were stiffer than the PAV-aged binder. However, for cells 34 and 35 the extracted binders were softer than the PAV-aged binder. This was more pronounced for cell 35 binder. It is not clear if this trend is related to the presence of polymer modifiers in the PG -34 and -40 binders.

The $|G*|$ master curves confirm the trends observed in the limiting temperature analysis. However, significant differences between field and laboratory-aged binders are noticed in the phase angle master curves. For the unmodified binder in cell 33, the differences were minimal. For the modified binders in cells 34 and 35 the plateau seen in the PAV-aged binders disappears for the recovered binders, which show significantly higher phase angles in the low frequency (high temperature) region. It is not clear if this is a consequence of the degradation of the polymer network due to aging or due to the recovery and extraction process.

At low temperatures, the stiffness and m-value limiting temperatures for all three cells were lower for the PAV-aged binders than the recovered binders, which may indicate more aging in the field binders. The most significant change, 15.2°C, is observed in the m-value limiting temperatures for the PG -40 binder which clearly indicates a substantial change in the relaxation properties of the recovered binder compared to the laboratory aged binder in spite of the less significant change in stiffness. The T_{cr} calculated from the BBR creep data and the DENT strength data matched reasonably well in some cases the BBR and DTT limiting temperatures without the use of the binder – mixture conversion factor, the so called pavement constant, which indicates that a revision of the PC concept may be necessary. The comparison of the stiffness curves confirms the trend observed in the limiting temperature analysis that for all three cells the extracted binders were always stiffer than the PAV-aged binders. The figures also show the significant reduction in the slope of the stiffness curves for the recovered binders compared to the PAV-aged binder, confirming the difference in the m-value limiting temperatures.

The fracture toughness experiments found no significant differences between the binders recovered from the different layers and between the recovered binders and the PAV-aged binder for cell 33. However, for cell 34 and 35 the PAV-aged binder had a higher toughness than the

recovered binders at -24°C. For cell 35 the top layer had a lower K_{IC} value than the middle layer, which in turn is lower than the bottom layer value, which may indicate higher aging effects in the top layer. It was also noted that the K_{IC} values at -24°C for the top layer of cell 34 and cell 35 are very similar, which indicates similar fracture resistance in spite of the different grade of the original binders.

The analyses performed in this research indicate that there are differences in the properties of binders recovered from various locations within the thickness of a pavement. For most situations the top layer seemed to age more than the other layers. The difference in properties between the laboratory-aged and the recovered binders were significant for the polymer modified binders used in cells 34 and 35, in particular for the PG-40 binder.

CHAPTER 4

Data Analysis

Objectives

In the previous two chapters the fracture properties of the asphalt binders and asphalt mixtures from the three MnROAD cells were determined. In this chapter correlations between the binder and mixture fracture toughness and between the fracture properties and the cells field performance are investigated.

Fracture Toughness Investigation

Fracture tests were performed on the extracted asphalt binders and on the field asphalt mixtures using the DENT and the SCB test procedures, respectively. In addition, DENT tests were also performed on the PAV-aged original binders used in the construction of the three cells. A summary of the fracture toughness results is shown in Table 4.1. For comparison purposes, the values are also plotted in Figures 4.1 to 4.6.

Table 4.1. Toughness values for asphalt binders and mixtures

Source	Binder				Mixture					
	T_1 (ºC)	K_{IC} (KPa.m$^{0.5}$)	T_2 (ºC)	K_{IC} (KPa.m$^{0.5}$)	T_1 (ºC)	K_{IC} (KPa.m$^{0.5}$)	T_2 (ºC)	K_{IC} (KPa.m$^{0.5}$)	T_3 (ºC)	K_{IC} (KPa.m$^{0.5}$)
33-T		48		67		740		820		780
33-M	-12	63	-18	63	-18	770	-24	910	-30	810
33-B		70		69		770		780		820
34-T		85		88		880		950		900
34-M	-18	123	-24	88	-24	900	-30	970	-36	930
34-B		91		68		900		1020		960
35-T		76		100		800		820		830
35-M	-24	105	-28	120	-24	800	-30	850	-36	970
35-B		113		140		740		860		960
33PAV	-18	67	-24	54						
34PAV	-24	133	-28	132						
35PAV	-28	168								

Figure 4.1 indicates that for cell 33 there are no significant differences between the binders recovered from the different layers and the PAV-aged binder at -18°C. However, the fracture toughness increases from top to bottom at -12°C.
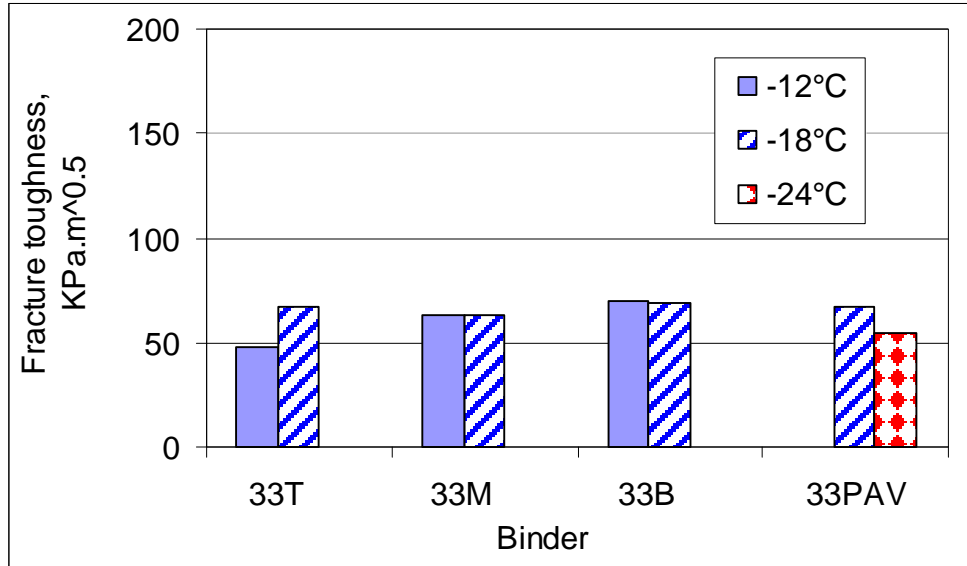
Figure 4.1. Fracture toughness - cell 33 asphalt binders

Figure 4.2 shows there are no significant difference between the three locations for the mixtures from cell 33. Very small variation in the fracture toughness with temperature is also noticed for this cell.
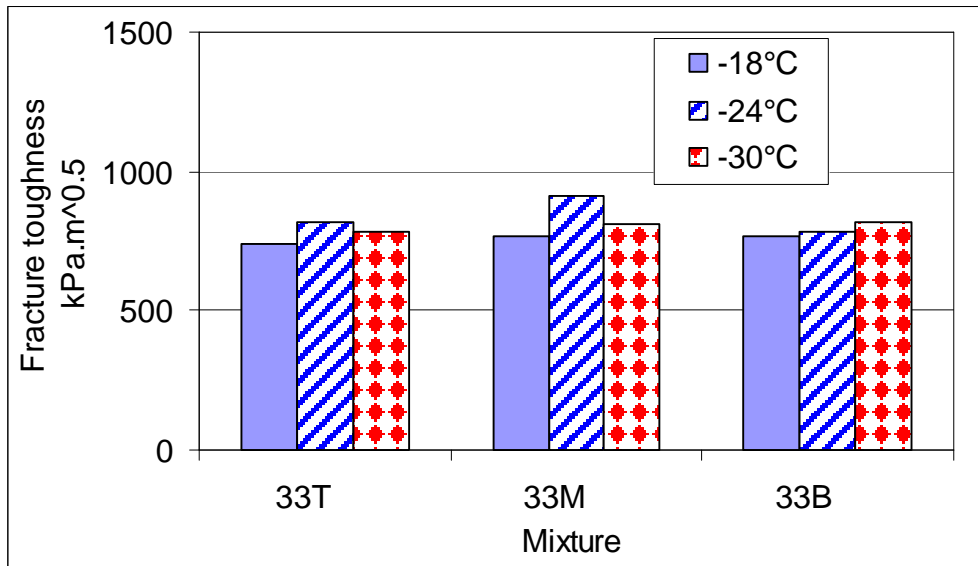
Figure 4.2. Fracture toughness - cell 33 asphalt mixtures

Figure 4.3 indicates that for cell 34 the PAV-aged binder has a higher toughness than the recovered binders at -24°C. There is no obvious trend with layers for the toughness of binders extracted from cell 34. The binders from the middle and the bottom layers appear to have higher toughness than the top layer at -18°C. However, the bottom layer has the smallest toughness at -24°C, while the top layer and middle layer have similar toughness values.
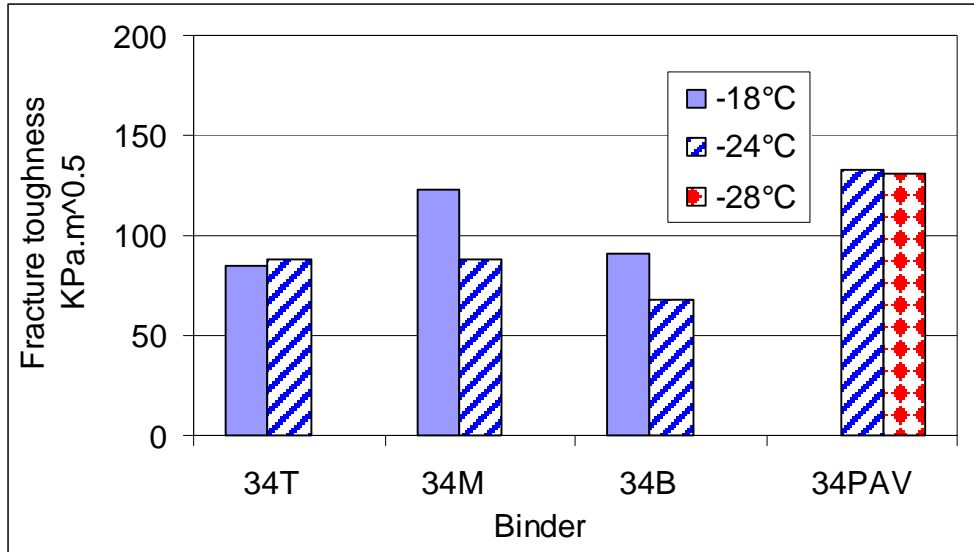
Figure 4.3. Fracture toughness - cell 34 asphalt binders

The toughness data for the mixtures from cell 34 plotted in figure 4.4 shows a clear trend with layer location. At -30°C and -36°C the toughness increases with layer depth. The top layer shows the smallest toughness at -18°C, while the middle and bottom layers have very similar values.
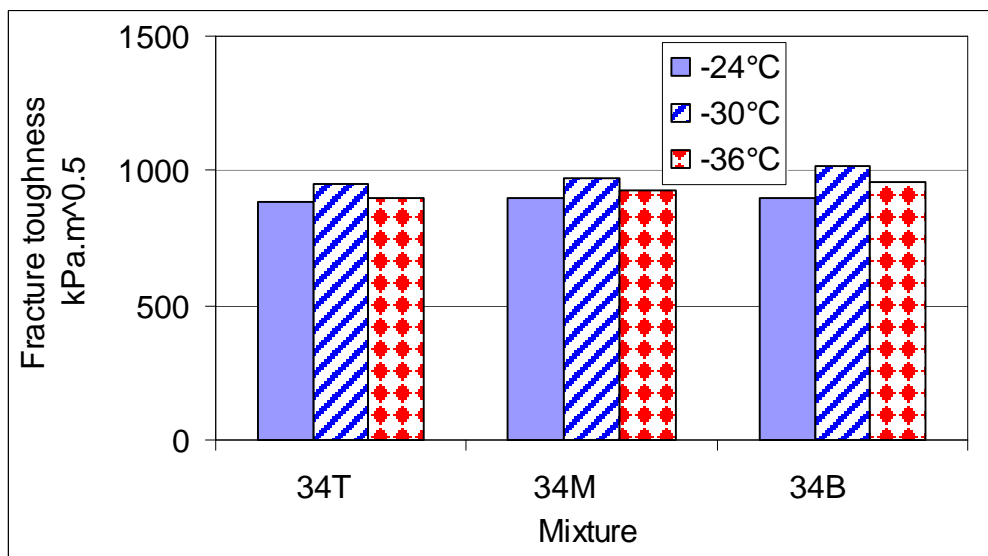
Figure 4.4. Fracture toughness - cell 34 asphalt mixtures

The data in figure 4.5 indicates that for cell 35 the PAV-aged binder also has a higher K_{IC} than the recovered binders. There is a clear trend for the binder toughness for cell 35: the toughness increases with the layer depth from top to bottom for both test temperatures. This may indicate higher aging effects in the top layer and the evolution of aging with pavement depth.
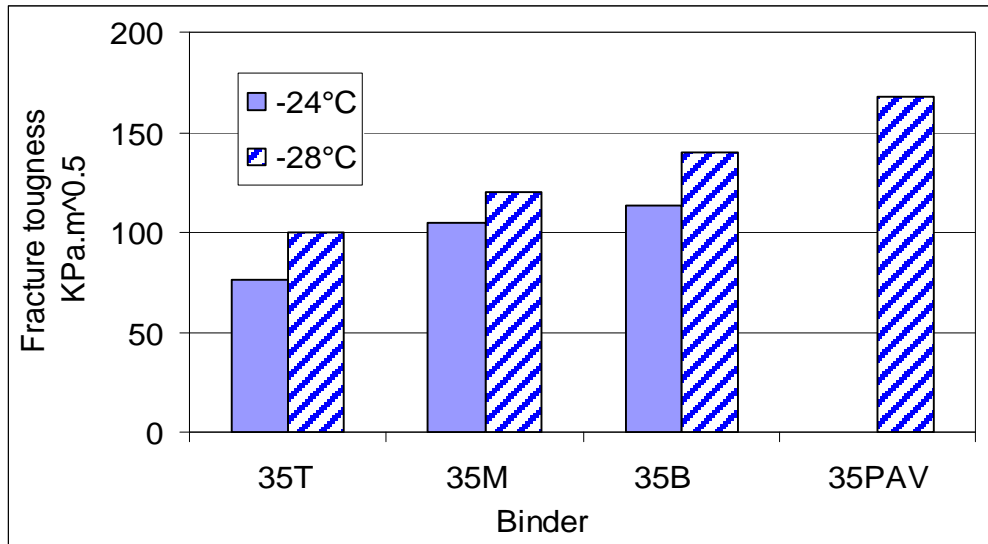
Figure 4.5. Fracture toughness - cell 35 asphalt binders

Figure 4.6 indicates that the mixture in the top layer has the smallest toughness at -30°C and -36°C; the middle and the bottom have very similar values, which may indicate higher aging effects in the top layer. However, the bottom layer has the lowest toughness at -24°C and the other two layers have similar values at this temperature.
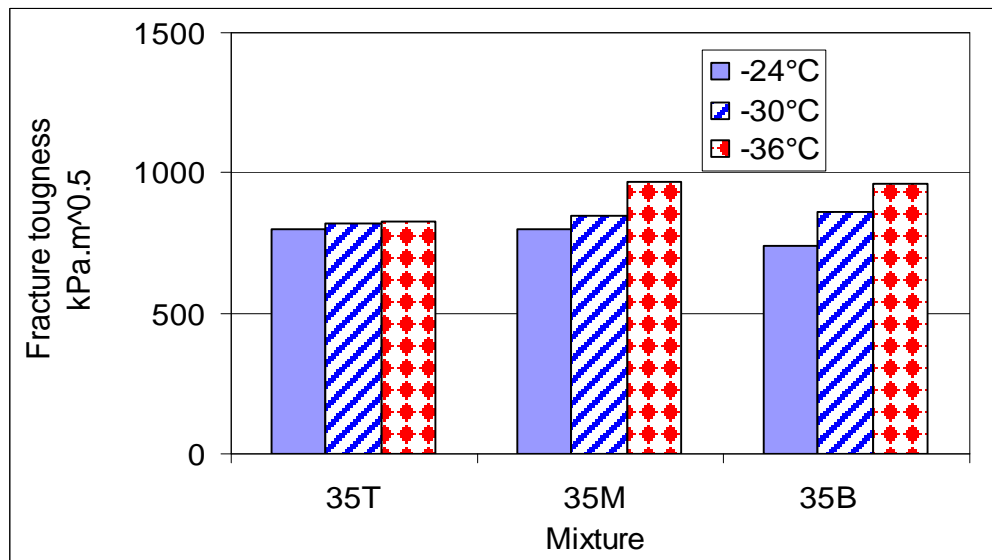
Figure 4.6. Fracture toughness - cell 35 asphalt mixtures

A summary of the data indicates that the fracture toughness of the recovered binders from cell 33 does not vary significantly with layer depth at -18ºC; this trend is also observed for the mixture toughness data. A similar trend is observed for the recovered binders from cell 34; however, the mixture data from the same cell indicates a clear toughness variation with location, with the lowest toughness in the top layer. The recovered asphalt binders' data and the mixtures data from cell 35 both indicate that the lowest toughness is measured in the top layer, which may indicate that more aging occurring at the surface of the pavement.

The fracture toughness describes the ability of the material to resist cracking. In this research it was found from that the ability of cracking resistance of the asphalt binder and mixture depends on the binder grade. The fracture test on binders resulted in fracture toughness values between 60 and 70 $KPa.m^{0.5}$ for most binders recovered from cell 33, between 80 and 100 $KPa.m^{0.5}$ for most binders from cell 34, and between 80 to 120 $KPa.m^{0.5}$ for most binders from cell 35. For the mixtures for most of the samples tested the values ranged as follows: 750 to 800 $KPa.m^{0.5}$ for cell 33, 900 to 1000 $KPa.m^{0.5}$ for cell 34, and 800 to 1000 $KPa.m^{0.5}$ for cell 35. This illustrates that the asphalt binders and mixtures from cell 33 have the lowest toughness values compared with the other two cells, in which polymer modified binders were used, that indicates that cell 33 is of the lowest cracking resistance. It is also noted that the toughness values at -24°C for the top layer of cell 34 and cell 35 are very similar, which may indicate similar fracture resistance in spite of the different grade of the original binders. Overall the fracture toughness values for the mixtures from cells 34 and 35, respectively, are very similar at -30°C and -36°C, indicating similar cracking resistance for these two materials.

Correlation of Experimental Results to Field Performance

Field performance data was obtained from the MnROAD research group to develop correlations between the experimental data and the field distresses. The three cells show very little low temperature distresses. The first cracks developed in February 2003. Except for cell 33, these cracks do not exhibit a "typical" thermal cracking pattern, which runs perpendicular to the centerline of lanes and across the entire width of both lanes. These cracks are more random in nature. Table 4.2 shows the amount of transverse cracks through May, 2005.

Table 4.2. Field Transverse Cracking

Cell	80K Inside Lane		102K Outside Lane	
	Number of cracks	**Linear Feet**	**Number of cracks**	**Linear Feet**
33	15	111	5	60
34	2	8	0	0
35	95	399	129	542

The data indicates that cell 33 (PG 58-28) has 6 full-width transverse cracks in both lanes. No cracks were observed in cell 34 (PG 58-34) in the 102K outside lane and 2 cracks were observed in the 80k inside lane. Many small transverse-like cracks were observed in cell 35 (PG 58-40). It is not clear if these cracks are the result of low-temperature stresses or were induced by traffic loading. Figures 4.7 to 4.9 show the typical field condition for each cell. These results indicate the superior field performance of the PG 58-34 binder, which is consistent with the experimental results.

Figure 4.7. Field condition for cell 33

Figure 4.8. Field condition for cell 34

Figure 4.9. Field condition for cell 35

CHAPTER 5

Conclusions and Recommendations

Conclusions

A number of conclusions can be drawn from the research performed in this study. The analysis of the experimental results from the SCB fracture tests performed on the field samples cored from cells 33, 34, and 35 indicated that the fracture energy of the field samples is significantly affected by the temperature and the type of binder used, while the fracture toughness of the field samples is significantly affected only by the type of binder used. The field samples and the laboratory specimens (tested in a previous study) are statistically different with respect to both the fracture toughness and the fracture energy; the fracture energy of the field samples is lower than the fracture energy of the laboratory specimens and the fracture toughness of the field samples is lower than the fracture energy of the laboratory specimens. However, the evolutions of the fracture toughness and fracture energy with type of binder and temperature are similar for the field samples and laboratory specimens. The difference in properties with the location within the pavement did not indicate a consistent pattern although in most cases the surface seemed to be less crack-resistant (possibly indicating more aging) than the middle and the bottom layer.

The analysis of the experimental data obtained from tests performed on the binders recovered from cores taken out of MnRoad cells 33, 34 and 35 and on the laboratory-aged original binders used in the construction of the three cells indicated that the properties of the field binders are different than the laboratory-aged binders. In particular, significant differences are noticed in the phase angle master curves. It is not clear if this is a consequence of the degradation of the polymer network due to aging or due to the recovery and extraction process. At low temperatures, the most significant change, 15.2°C, is observed in the m-value limiting temperatures for the PG -40 binder, which clearly indicates a substantial change in the relaxation properties of the recovered binder compared to the laboratory-aged binder in spite of the less significant change in stiffness. The difference in properties with the location within the pavement did not indicate a consistent pattern although in most cases the surface seemed to be stiffer (possibly indicating more aging) than the middle and the bottom layer.

The small number of thermal cracks in the three cells limited the development of correlations between the experimental data and the field performance. The experimental data indicates that both the binders and the mixtures used in cells 34 and 35 have superior properties compared to cell 33 materials, which is also observed in the field.

Recommendations

The research performed in this study indicates that the fracture tests performed on asphalt binders and asphalt mixtures have the potential to predict the field performance of asphalt pavements with respect to thermal cracking. The binder results confirm the predictions of the current performance grading system; however, it appears that the fracture resistance of the PG-34 asphalt mixture is better than the fracture resistance of the PG-40 mixtures, which is the opposite of what the PG system predicts.

More research is needed to validate the conclusions of this work and to address a number of issues that are still unclear:

- Refine the analysis as more thermal cracking data becomes available. It is important to capture as accurately as possible the time and temperature when the cracks propagate or become visible.

- Extend the analysis to more cells or pavements for which materials are available and perform the tests described in this study to create a comprehensive data base. It is important to include similar mixtures prepared with similar PG asphalt binders.

- Perform a chemical analysis of the extracted binders to further investigate the significant differences in phase angle and m-value between the extracted and the laboratory aged binders.

- Improve the specimen preparation method for the fracture toughness test performed on asphalt binders. The mixture fracture toughness values were typically 10 to 12 times higher than the binder fracture toughness, which indicate that the binder fracture toughness may be a reasonable predictor of mixture toughness.

REFERENCES

(1)   Lim, I. L., Johnston, I. W. and Choi, S.K., "Stress Intensity factors for Semi-Circular Specimens under Three-Point Bending," *Engineering Fracture Mechanics*, vol. 44, no. 3, (1993), 363-382.

(2)   RILEM Technical Committee 50-FMC, "Determination of the Fracture Energy of Mortar and Concrete by Means of Three-point Bend Tests on Notched Beams," *Materials and Structures*, no. 106, (Jul-Aug 1985), 285-290.

(3)   Li, X., Marasteanu, M.O., "Evaluation of the Low Temperature Fracture Resistance of Asphalt Mixtures Using the Semi Circular Bend Test," *Journal of the Association of Asphalt Paving Technologists*, vol. 73, (2004), 401-426.

(4)   Li, X. *Investigation of the Fracture Resistance of Asphalt Mixtures at Low Temperatures with a Semi Circular Bend (SCB) Test*. (Ph.D. Thesis, University of Minnesota, 2005).

(5)   American Association of State Highway and Transportation Officials (AASHTO), *Standard Method of Test for Quantitative Extraction of Asphalt Binder from Hot Mix Asphalt*, AASHTO Designation: T 164-05i, ASTM Designation: D 2172-01.

(6)   Strategic Highway Research Program, *Extraction and recovery of asphalt cement for rheological testing*, SHRP-A-370, Binder Characterization and Evaluation, Vol. 4: Test Methods, Appendix E, National Research Council, Washington, DC 1994.

(7)   American Association of State Highway and Transportation Officials (AASHTO), *Standard Method of Test for Effect of Heat and Air on a Moving Film of Asphalt (Rolling Thin-Film Oven Test)*, Designation T 240-00, "Standard Specifications for Transportation Materials and Methods of Sampling and Testing, Part 2B: Tests," 22nd Edition, 2002.

(8)   American Association of State Highway and Transportation Officials (AASHTO), *Standard Practice for Accelerated Aging of Asphalt Binder Using a Pressurized Aging Vessel (PAV)*, Designation R 28-02, "Standard Specifications for Transportation Materials and Methods of Sampling and Testing, Part 1B: Specifications," 22nd Edition, 2002.

(9)   American Association of State Highway and Transportation Officials (AASHTO), *Standard Method of Test for Determining the Rheological Properties of Asphalt Binder*

Using a Dynamic Shear Rheometer (DSR), Designation T 315-02, "Standard Specifications for Transportation Materials and Methods of Sampling and Testing, Part 2B: Tests," 22nd Edition, 2002.

(10) American Association of State Highway and Transportation Officials (AASHTO), *Standard Method of Test for Determining the Flexural Creep Stiffness of Asphalt Binder Using the Bending Beam Rheometer (BBR)*, Designation T 313-02, "Standard Specifications for Transportation Materials and Methods of Sampling and Testing, Part 2B: Tests," 22nd Edition, 2002.

(11) American Association of State Highway and Transportation Officials (AASHTO), *Standard Method of Test for Determining the Fracture Properties of Asphalt Binder in Direct Tension (DT)*, Designation T 314-02, "Standard Specifications for Transportation Materials and Methods of Sampling and Testing, Part 2B: Tests," 22nd Edition, 2002.

(12) Gilles G. Gauthier. *Evaluation of Low-Temperature Fracture Properties of Asphalt Binder*. (Master Thesis, The Pennsylvania State University, July 2003).

(13) Marasteanu, M. O. and Anderson, D. A., "Improved Model for Bitumen Rheological Characterization", *Eurobitume Workshop on Performance Related Properties for Bituminous Binders*, Luxembourg, 1999

(14) American Association of State Highway and Transportation Officials (AASHTO), *Standard Specification for Performance Graded Asphalt Binder*, Designation: MP1a-02, "AASHTO Provisional Standards," May 2002 Edition, 2002.

(15) Shenoy, A., "Single-Event Cracking Temperature of Asphalt Pavements Directly from the Bending Beam Rheometer Data," *Journal of Transportation Engineering*, vol. 128, no. 5, (2002).

(16) Anderson T.L. *Fracture Mechanics, Fundamentals and Application* (CRC Press, Second Edition, 1995).